FSHIP2 regulates epithelial cell polarity through its lipid product, which binds to Dlg1, a pathway subverted by hepatitis C virus core protein

Aline Awad[a,b], Sokhavuth Sar[a,b], Ronan Barré[c], Clotilde Cariven[c], Mickael Marin[a,b], Jean Pierre Salles[c], Christophe Erneux[d], Didier Samuel[a,b,e], and Ama Gassama-Diagne[a,b]

[a]Université Paris-Sud, UMR-S 785, F-94800 Villejuif, France; [b]Inserm, Unité 785, F-94800 Villejuif, France; [c]Département Lipoprotéines et Médiateurs Lipidiques, Centre de Physiopathologie de Toulouse Purpan, Université Toulouse III Paul-Sabatier, INSERM Unité 563, 31059 Toulouse Cedex, France; [d]Institut de Recherche Interdisciplinaire, Université Libre de Bruxelles, Campus Erasme, 1070 Brussels, Belgium; [e]AP-HP Hôpital Paul Brousse, Centre Hépato-Biliaire, F-94800 Villejuif, France

ABSTRACT **The main targets of hepatitis C virus (HCV) are hepatocytes, the highly polarized cells of the liver, and all the steps of its life cycle are tightly dependent on host lipid metabolism. The interplay between polarity and lipid metabolism in HCV infection has been poorly investigated. Signaling lipids, such as phosphoinositides (PIs), play a vital role in polarity, which depends on the distribution and expression of PI kinases and PI phosphatases. In this study, we report that HCV core protein, expressed in Huh7 and Madin–Darby canine kidney (MDCK) cells, disrupts apicobasal polarity. This is associated with decreased expression of the polarity protein Dlg1 and the PI phosphatase SHIP2, which converts phosphatidylinositol 3,4,5-trisphosphate into phosphatidylinositol 4,5-bisphosphate (PtdIns(3,4)P2). SHIP2 is mainly localized at the basolateral membrane of polarized MDCK cells. In addition, PtdIns(3,4)P2 is able to bind to Dlg1. SHIP2 small interfering RNA or its catalytically dead mutant disrupts apicobasal polarity, similar to HCV core. In core-expressing cells, RhoA activity is inhibited, whereas Rac1 is activated. Of interest, SHIP2 expression rescues polarity, RhoA activation, and restricted core level in MDCK cells. We conclude that SHIP2 is an important regulator of polarity, which is subverted by HCV in epithelial cells. It is suggested that SHIP2 could be a promising target for anti-HCV treatment.**

Monitoring Editor
Alpha Yap
University of Queensland

Received: Aug 24, 2012
Revised: Apr 22, 2013
Accepted: May 16, 2013

INTRODUCTION

Hepatitis C virus (HCV) chronically infects >170 million people worldwide, and complications from HCV infection are the leading indication for liver transplantation. There is no vaccine to protect against HCV infection. Although major improvement has been recently achieved regarding treatment of HCV infection, there is already evidence for emergence of genotypic resistance due to the high genetic variability of the HCV RNA genome. This will lead in the future to the design of combination therapeutic agents targeting different HCV proteins, such as HCV proteases and HCV polymerase (Bartenschlager *et al.*, 2011; Rice, 2011). It will also be important to design therapies targeting cellular proteins. Thus identification of the cellular signaling pathways subverted by HCV to induce pathogenesis may have profound effect on therapeutics.

HCV has a single-stranded RNA genome encoding for a polyprotein that is cleaved by cellular and viral proteases to produce the viral structural proteins, the nucleocapsid (core) and envelope glycoproteins E1 and E2, p7, and the nonstructural (NS) proteins NS2, NS3, NS4A, NS4B, NS5A, and NS5B (Moradpour *et al.*, 2007; Bartenschlager *et al.*, 2011). Each step of the HCV replication cycle is tightly dependent on host cell lipid metabolism, and indeed liver steatosis is a common histological feature of HCV infection

This article was published online ahead of print in MBoC in Press (http://www.molbiolcell.org/cgi/doi/10.1091/mbc.E12-08-0626) on May 22, 2013.

The authors declare no competing financial interests.

Address correspondence to: Ama Gassama-Diagne (ama.gassama@inserm.fr).

Abbreviations used: Cyt, cytosol; Dlg1, disks large homologue 1; ECM, extracellular matrix; GP135, glycoprotein 135; H, homogenate; HCV, hepatitis C virus; Huh7, human heptocarcinoma; Mb, membrane; MDCK, Madin–Darby canine kidney; PtdIns, phosphatidylinositol; SHIP2, SH2 domain–containing inositol phosphate 5-phosphatase 2.

(Barba *et al.*, 1997). The lipid droplets (LDs) accumulated in HCV-infected cells play a central role in the production of infectious particles and participate in virus assembly (Miyanari *et al.*, 2007). LDs are dynamic functional organelles that consist of a hydrophobic core of neutral lipids surrounded by a monolayer of phospholipids, including phosphoinositides (Martin and Parton, 2006; Olofsson *et al.*, 2009).

The phosphoinositides represent a minor part of membrane phospholipids. Their metabolism is highly active and accurately controlled by a number of specific kinases, phosphatases, and phospholipases in discrete membrane domains, however, and this makes them master regulators of a number of fundamental biological processes, including cell polarization (Gassama-Diagne and Payrastre, 2009; Shewan *et al.*, 2011). Phosphatidylinositol 3,4,5-trisphosphate (PtdIns(3,4,5)P3) is a key mediator of intracellular signaling, generated by the class I phosphatidylinositol 3-kinase (PI3K; Cantley, 2002). We previously demonstrated that PI3K and PtdIns(3,4,5)P3 build the basolateral membrane (Gassama-Diagne *et al.*, 2006), whereas 3-phosphatase and tensin homologue (PTEN), which dephosphorylates PtdIns(3,4,5)P3 to phosphatidylinositol 4,5-bisphosphate (PtdIns(4,5)P2), generates the apical membrane (Martin-Belmonte *et al.*, 2007). These studies helped to demonstrate spatial restriction of the phosphoinositides for cell polarization (Comer and Parent, 2007).

Cell polarity is important to maintain structure and function of epithelia and establishes a protective barrier against infections by pathogens. A large number of pathogens target cell polarity proteins to attach and invade epithelial cells, however, leading to loss of polarity and development of pathogenesis as infectious diseases and cancers (Kazmierczak *et al.*, 2001; Muthuswamy and Xue, 2012).

HCV primarily infects the liver, a highly polarized epithelium (Rice, 2011). Several reports indicate the importance of tight junction proteins in HCV entry into host cells (Ploss *et al.*, 2009; Bartenschlager *et al.*, 2011). HCV infection reduces hepatocellular polarity (Liu *et al.*, 2009; Mee *et al.*, 2010) and promotes alterations of polarity-associated proteins (Benedicto *et al.*, 2008). Nevertheless, few data in the literature concern the relation between cell polarization and HCV life cycle (Mee *et al.*, 2008, 2009; Snooks *et al.*, 2008; Benedicto *et al.*, 2011).

Studies show an intimate connection between HCV life cycle, lipid metabolism, and epithelial cell polarity, although the underlying mechanisms of this complex relationship are scarcely understood. Studies on the role of lipids in the HCV life cycle concern mostly the machinery of lipoproteins, and recent work describes the involvement of fatty acids and cholesterol biosynthesis (Kapadia and Chisari, 2005; Herker *et al.*, 2010; Alvisi *et al.*, 2011; Benedicto *et al.*, 2011; Roe *et al.*, 2011). Nevertheless, there are increasing reports that HCV targets host PI signaling and metabolism pathways in its infection cycle. The major studies identify a critical role of two isoforms of phosphatidylinositol 4-kinase (PI4K-IIIα and PI4K-IIIβ) and their lipid product, PtdIns4P, for HCV replication (Berger *et al.*, 2009, 2011; Borawski *et al.*, 2009; Trotard *et al.*, 2009; Reiss *et al.*, 2011; Bianco *et al.*, 2012).

Here we focus on another PI metabolizing enzyme, the SH2 domain–containing inositol phosphate 5-phosphatase 2 (SHIP2), which mainly dephosphorylates PtdIns(3,4,5)P3 to form PtdIns(3,4)P2 (Backers *et al.*, 2003). In unstimulated cells, SHIP2 has a perinuclear and cytoplasmic localization, whereas in serum-stimulated cells SHIP2 can be localized at the plasma membrane and at focal contacts. A phosphorylated form of SHIP2 was found in the nucleus and could potentially control PtdIns(4,5)P2 levels (Elong Edimo *et al.*, 2013). SHIP2 down-regulates insulin signaling and was proposed as a target in some diabetic models (Marion *et al.*, 2002) and obesity (Sleeman *et al.*, 2005). Its importance in some types of human skeletal dysplasia, such as opsismodysplasia (OMIM 258480), was recently reported (Huber *et al.*, 2013). Cellular roles proposed for SHIP2 include remodeling of actin structures, lamellipodia formation, cell adhesion, and spreading and receptor endocytosis whereas its role in epithelial cell polarity has not been investigated (Prasad *et al.*, 2001; Ooms *et al.*, 2009; Elong Edimo *et al.*, 2013).

Our study reveals localization of SHIP2 and it lipid product, PtdIns(3,4)P2, at the basolateral domain of polarized MDCK cells, where it plays a critical role in the establishment of apicobasal polarity. Using both Huh7.5 and Madin–Darby canine kidney (MDCK) cells stably transfected with HCV core, we demonstrate that HCV core targets a SHIP2 pathway to induce loss of apicobasal polarity.

RESULTS

HCV core protein is present at the basal membrane and disrupts apicobasal polarity

The HCV core protein is a structural component of the nucleocapsid and plays an essential function in HCV assembly and replication (Jones and McLauchlan, 2010). HCV core disrupts different cellular signaling pathways by interaction with various cellular proteins (Kunkel and Watowich, 2004; Boulant *et al.*, 2008; Jones and McLauchlan, 2010) and has been implicated in HCV-related pathogenesis, including steatosis (Moriya *et al.*, 1997; Perlemuter *et al.*, 2002) and carcinogenesis (Moriya *et al.*, 2001). We examined HCV core localization and cell morphogenesis in two different epithelial cell lines that stably express core protein. Huh7 is a human hepatoma cell line highly permissive for infectious HCV, but fails to fully polarize in culture. Therefore we chose to use MDCK cells grown in three-dimensional (3D) culture, which represents a unique model system for analysis of epithelial cell polarity in relatively physiological conditions. Even though MDCK cells do not present the complex polarized phenotype of hepatocytes, they can represent a valuable model system in which to study the molecular mechanisms that connect HCV to cell polarity.

First, the presence of core protein was validated in the two cell lines by Western blotting (Figure 1A). Next Huh7 core cells were grown on filters and analyzed by confocal microscopy (Figure 1B). In these polarization conditions, core is mainly present in the cytoplasm, and the *XZ* section indicates its enrichment in the basal domain. In comparison to control cells, disorganization of β-catenin signal is observed in core-containing cells associated with a reduction of cell thickness from 9.7 to 8.1 μm, as indicated on the right of the *XZ* pictures (Figure 1B). Similar results are obtained using MDCK core cells, and analysis of *XZ* sections indicates basal localization of the core and ~30% reduction in cell thickness (from 10.4 to 7.3 μm) compared with polarized control cells (Figure 1B). The complete *Z*-series is given in Supplemental Figures S1 and S2 for Huh7 and MDCK cells, respectively. We performed subcellular fractionation of MDCK core cells using ultracentrifugation and compared with the result with control MDCK cells. Figure 1C shows that core protein is largely present in the membrane fraction, whereas a minor part is found in the cytosol. β-Catenin is found mainly in the membrane, although the level in the cytosol is higher than in control cells, probably due to the presence of core protein.

To gain more insight into the role of HCV core in cell morphogenesis and polarity, we grew MDCK core cells in 3D on

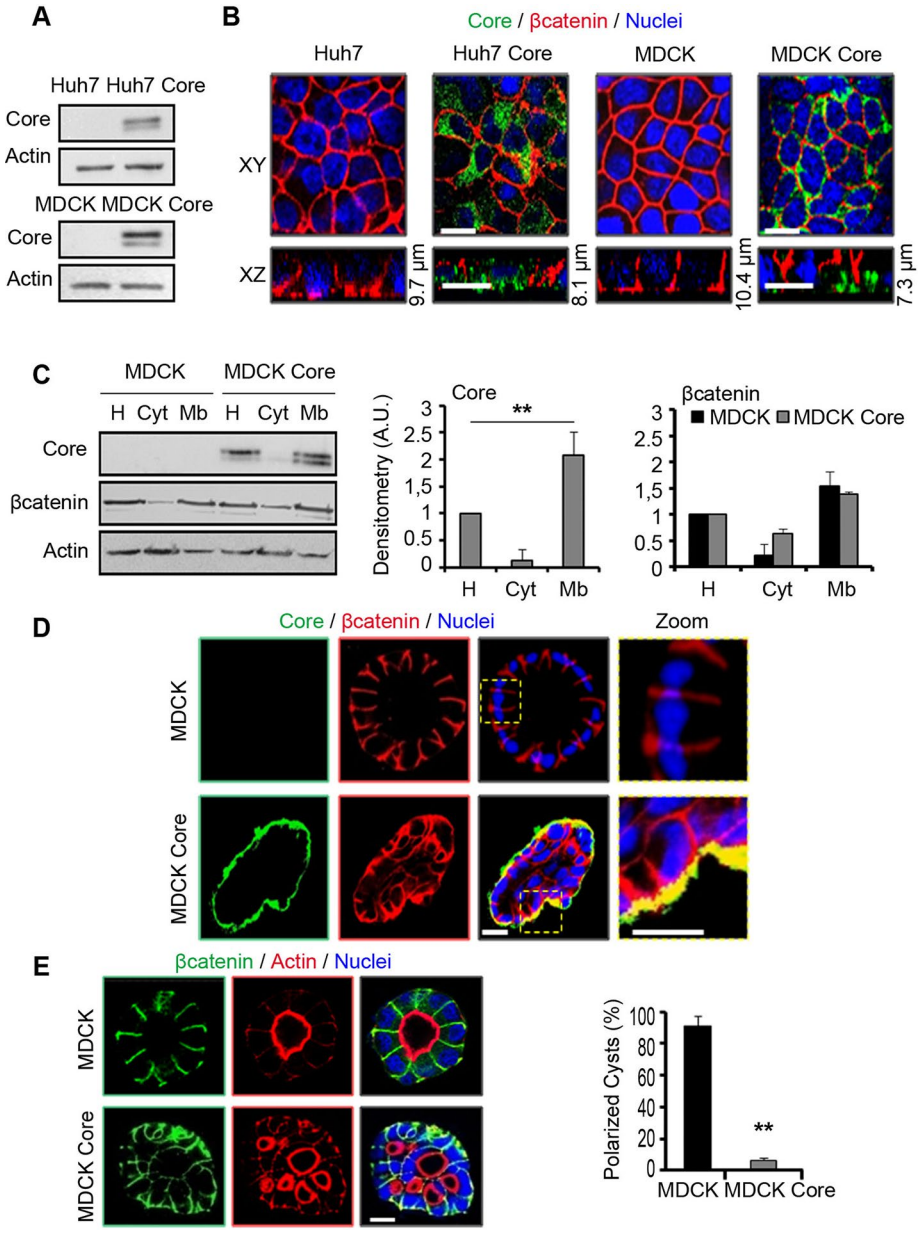

FIGURE 1: HCV core protein is present mainly at the basal membrane and disrupts polarity. (A) Immunoblot analysis of core protein stably expressed in Huh7 and MDCK cells compared with nontransfected cells used as control. Actin is used as loading control. (B) Huh7 and MDCK cells, expressing or not expressing HCV core protein, were grown on filters as a monolayer for 3 d and then fixed, stained for core (green) and β-catenin (red) as indicated, and imaged by confocal microscopy. Nuclei were stained with Hoechst. *XY* and *XZ* sections are presented. Scale bar, 10 µm. (C) Homogenates (H) from MDCK and MDCK core cells grown for 3 d were submitted to ultracentrifugation at 100,000 × *g* to separate membrane (Mb) from cytosolic (Cyt) compartments and analyzed by immunoblotting for core, β-catenin, and actin used as loading control. The densitometry analysis normalized to actin from three independent experiments is represented in arbitrary units (A.U.). Error bars, SD. $^{**}p < 0.001$. (D) MDCK cells expressing or not expressing HCV core protein were grown in Matrigel for 4 d to form cysts and then stained for core (green), β-catenin (red), and nuclei (blue) with Hoechst as indicated. Single confocal section through the middle of a cyst. Right, a zoom. Scale bar, 10 µm. (E) Cells in D stained for β-catenin (green), actin (red), and nuclei with Hoechst (blue). Single confocal section through the middle of a cyst. Scale bar, 10 µm. Percentage of polarized cysts with normal single lumen detected with actin staining is presented as a histogram. We counted 250 cysts from control and MDCK core cells in three independent experiments. Error bars, SD. $^{**}p < 0.001$.

Matrigel to form cysts. (Figure 1D). Immunofluorescence analysis shows prominent basal localization of core at the cell–extracellular matrix (ECM) contact and partial colocalization with β-catenin. Indeed, β-catenin signal is profoundly disorganized, and an important signal is present at the cell–ECM contacts of a discoidal structure. In control cells, β-catenin signal is present essentially at cell–cell contacts of cysts with a spherical monolayer (Figure 1D). We further analyzed polarity status in these MDCK core cysts by staining actin to visualize the apical domain (Figure 1E). As expected, control MDCK cysts formed a central single lumen represented with actin staining, whereas MDCK core cells formed multilumen cysts. About 250 cysts were analyzed, and data are presented as histograms (Figure 1E), indicating that core protein has a dramatic effect on cell polarity, with >90% of cysts presenting multilumens.

HCV core affects expression and localization of the polarity proteins

On the basis of the observed effects of core on cell morphogenesis, we chose to analyze two master regulators of basolateral polarity, Scribble and Dlg1 (Bryant and Mostov, 2008), which were localized in adherent junctions, as shown in control MDCK cysts (Figure 2A). Dlg1 staining was reduced in cell–cell contacts in MDCK core cysts, and a faint punctuate signal was observed, whereas less reduction of Scribble was observed, and instead it was delocalized to ECM contacts (Figure 2A), as observed for β-catenin in Figure 1D. Costaining of Dlg1 or Scribble with core protein is presented in Figure 2B. Here again, as observed in Figure 1D, core protein accumulates at the membrane at ECM contact, where colocalization with Scribble is observed. Immunoblot analysis of the cell lysates confirmed significant reduction of Dlg1 expression in MDCK core cyst compared with controls, whereas Scribble expression was not significantly decreased (Figure 2C). These immunoblot data were validated using Huh7 cells (Figure 2D). We analyzed the Par3 protein, another master regulator of polarity located in tight junctions (Bryant and Mostov, 2008), and observed no noticeable change in its expression (Supplemental Figure S3A). Redistribution of E-cadherin and ZO-1 was also observed in MDCK core cysts (Supplemental Figure S3B). Together the data indicate that HCV core protein targets differently the expression and localization of polarity proteins.

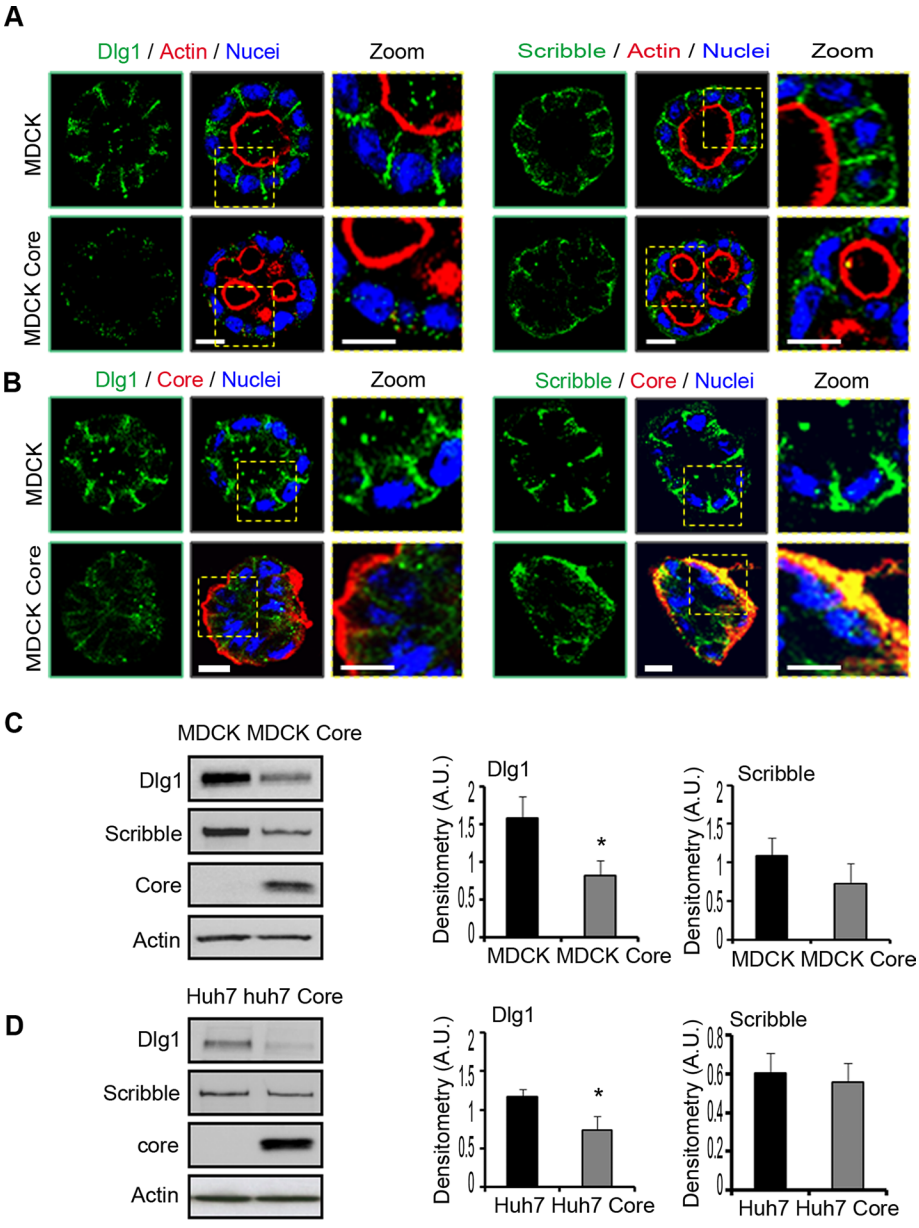

FIGURE 2: Dlg1 and Scribble are down-expressed in Huh7 and MDCK cells expressing HCV core protein. (A) MDCK cells expressing or not expressing HCV core protein were grown in Matrigel for 4 d to form cysts and stained for Dlg1 or Scribble (green) and actin (red) as indicated. Nuclei were stained with Hoechst (blue). Single confocal section through the middle of a cyst. Right, a zoom. Scale bar, 10 μm. (B) Cells in A stained for Dlg1 or Scribble (green) and core (red) as indicated. Nuclei were stained with Hoechst (blue). Single confocal section through the middle of a cyst. Right, a zoom. Scale bar, 10 μm. (C) The lysates of cells grown as in A analyzed by immunoblotting with antibodies to Dlg1, Scribble, and actin as loading control. Densitometry analysis normalized to actin from four independent experiments is represented in arbitrary units (A.U.) in histograms. Error bars, SD. *$p < 0.05$. (D) Huh7 cells expressing or not expressing HCV core protein were grown for 3 d and the cell lysates analyzed by immunoblotting toDlg1, Scribble, and actin as loading control. Densitometry analysis normalized to actin from three independent experiments is represented in arbitrary units (A.U.) in histograms. Error bars, SD. *$p < 0.05$.

SHIP2 and PtdIns(3,4)P2 are localized to the basal membrane, and their levels are down-regulated by HCV core

PtdIns(3,4,5)P3 and PI3K regulate the formation of the basolateral plasma membrane, whereas PTEN antagonizes PI3K and produces PtdIns(4,5)P2 to generate lumen and the apical plasma membrane domain. Taken together, these studies helped to demonstrate the importance of spatial restriction of the PI for epithelial cell polarization (Comer and Parent, 2007). On the basis of the effect of HCV core on cell polarity, we hypothesized an eventual deregulation of the PtdIns-metabolizing enzymes by HCV to induce loss of polarity. We focus on SHIP2, a PI phosphatase that converts PtdIns(3,4,5)P3 to PtdIns(3,4)P2.

First, we examined the localization of SHIP2 in polarized MDCK cysts using a SHIP2 antibody. SHIP2 was found at the basal area at ECM–cell contacts, and, of interest, PtdIns(3,4)P2 was also present at the basal membrane even though some apical dots were observed (Figure 3A). These data were reinforced by transfection of MDCK cells with a green fluorescent protein (GFP) construct of SHIP2. The efficiency of the transfection was validated by immunoblot (Supplemental Figure S4A), and GFP SHIP2 was found mainly at the basal domain at ECM contact (Supplemental Figure S4, B and C). The localization of PtdIns(3,4)P2 was also examined using a yellow fluorescent protein–tandem pleckstrin homology domain protein (TAPP) probe (Supplemental Figure S4D). The probe comprised the pleckstrin homology domain of TAPP protein, which specifically binds to PtdIns(3,4)P2 (Wullschleger *et al.*, 2011). A signal was observed at the basal membrane; in contrast to data obtained with SHIP2 antibody, however, the signal was most diffuse in the cytoplasm. In addition, we analyzed the membrane localization of SHIP2 through subcellular fractionation using ultracentrifugation. Figure 3B shows that SHIP2 is enriched in the membrane fraction, with a minor part in the cytosol. Figure 3B shows a densitometry analysis of Western blot data. These results similar to the subcellular distribution of HCV core presented in Figure 1C.

We also examined the staining of SHIP2 and PtdIns(3,4)P2 in MDCK core cysts (Figure 3A, bottom). The two components are present at the basal membrane, and the staining of both is reduced in the multilumen MDCK core cysts. Decreased PtdIns(3,4)P2 signal is presented as histograms (Figure 3A). Immunoblot analysis of the cell lysates confirmed a significant reduction of SHIP2 expression in MDCK core cells (Figure 3C), as well as in Huh7 core cells (Figure 3D), compared with corresponding control cells. Examination of SHIP2 mRNA level via quantitative PCR in MDCK core cells indicates a decrease compared with control cells (Figure 3E).

SHIP2 regulates cell polarity through its enzymatic activity

Given the effects of HCV core on SHIP2 expression and the comparable localization of both proteins at the basal membrane

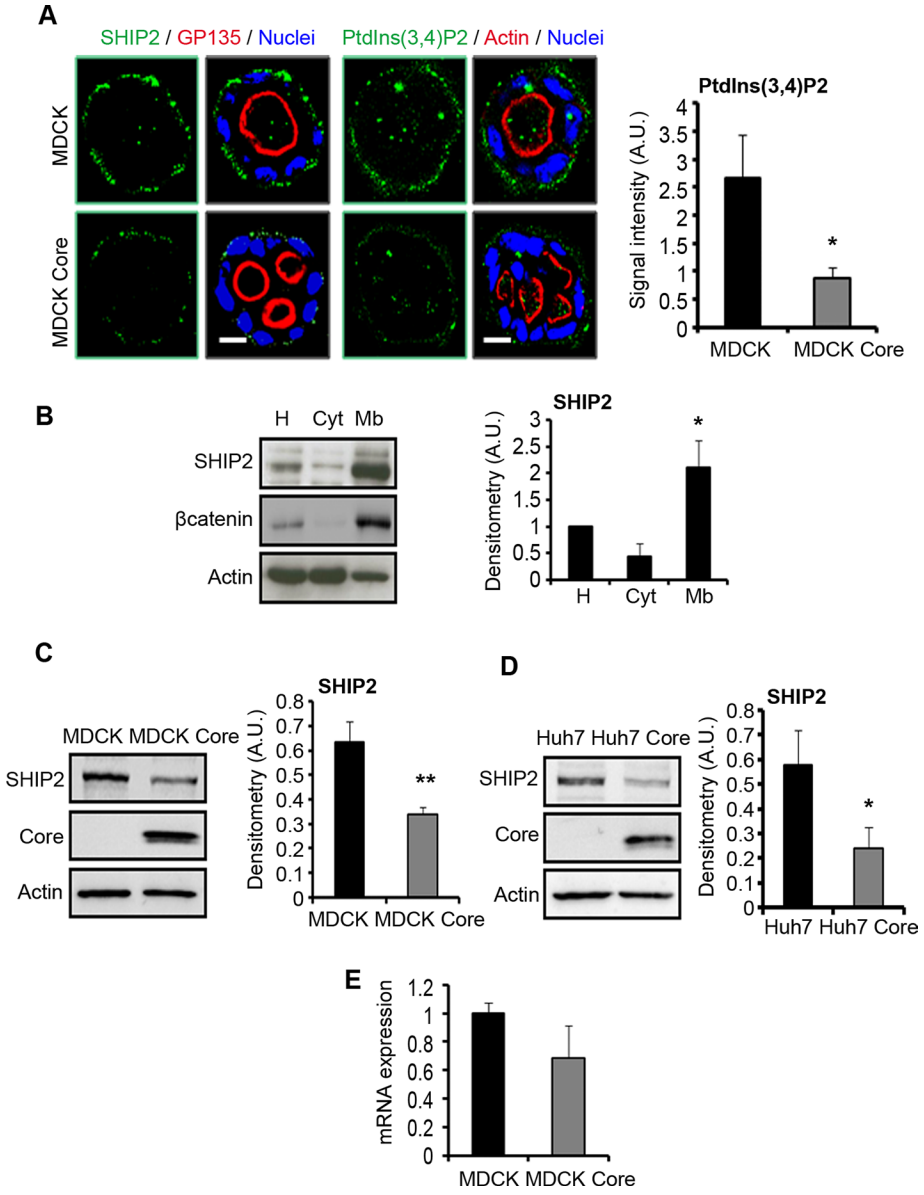

FIGURE 3: SHIP2 and PtdIns(3,4)P2 are both localized to the basal membrane of polarized cysts and down-regulated in the presence of HCV core protein. (A) MDCK cells expressing or not expressing HCV core protein were grown for 4 d in Matrigel and stained for SHIP2 or PtdIns(3,4)P2 (green) and actin (red) as indicated. Nuclei (blue) were stained with Hoechst. Single confocal section through the middle of cyst. Scale bar, 10 μm. Staining intensity of PtdIns(3,4)P2 was quantified with ImageJ from 10 cysts in three independent experiments and is presented in histograms. Error bars, SD. *$p < 0.05$. (B) Homogenates (H) from MDCK cells grown for 3 d were submitted to ultracentrifugation at 100, 000 × g to separate membrane (Mb) and cytosolic (Cyt) fractions and immunoblotted for SHIP2, β-catenin, and actin as loading control. Densitometry analysis normalized to actin from three independent experiments is represented in arbitrary units (A.U.) in a histogram. Error bars, SD. *$p < 0.05$. (C) Lysates of cells grown as in A analyzed by immunoblotting with anti-SHIP2 and core. Actin is used as loading control. The densitometry analysis normalized to actin from four independent experiments is represented in arbitrary units (A.U.) in histograms. Error bars, SD. **$p < 0.001$. (D) Huh7 cells expressing or not expressing HCV core protein were grown for 3 d and cell lysates analyzed by immunoblotting with anti-SHIP2 and anti-actin as loading control. The densitometry analysis normalized to actin from three independent experiments is represented in arbitrary units (A.U.) in histograms. Error bars, SD. *$p < 0.05$. (E) Total RNA from MDCK cells expressing or not expressing HCV core protein analyzed by quantitative PCR for SHIP2 expression and normalized to GAPDH (see *Materials and Methods*). Data are means ± SEM of three experiments done in triplicate.

(Figures 1 and 3), we hypothesized that SHIP2 could be a target for HCV to invade the basal surface and disrupt cell polarity. Thus we examined the potential role of SHIP2 on cell polarization using two different small interfering RNAs (siRNAs; si1 and si3) to deplete endogenous SHIP2. Immunoblot analysis indicated significant reduction of SHIP2 with both siRNAs, associated with reduction of Dlg1 and Scribble expression (Figure 4A). The effect of SHIP2 depletion on cell polarity was evaluated on MDCK cysts using si3, and the depletion of SHIP2 was further validated by SHIP2 staining (Figure 4B). We also analyzed the staining pattern of different polarity proteins (Figure 4B). Most of the SHIP2-depleted cysts presented multilumens, as visualized with both actin and the apical marker GP135 staining (Figure 4B). The basolateral polarity proteins β-catenin, Scribble, and Dlg1 were delocalized from the cell contacts, and the signal was severely reduced, as observed on immunoblot in Figure 4A. As observed with MDCK core cells, however, Par 3 protein expression was not affected in SHIP2 siRNA–treated cells (Supplemental Figure S5). Together these data suggested that SHIP2 is required for localization and expression of basolateral complex proteins to maintain cell morphogenesis.

Next we examined whether SHIP2 catalytic activity is required for its morphogenic effects. We transfected MDCK cells with a catalytically dead construct of SHIP2 that was Xpress tagged (D607A; Pesesse *et al.*, 2001; Zhang *et al.*, 2007) and grown in 3D on Matrigel. Transfection efficiency was analyzed by Western blot (Figure 4C), and the cysts were analyzed by confocal microscopy (Figure 4D). We observed a weaker signal for β-catenin and Scribble in the SHIP2 catalytic-dead cysts than in control cysts. Labeling of the apical glycoprotein GP135 and actin showed the presence of multilumens (Figure 4D) as observed with SHIP2 depletion using siRNA, indicating that SHIP2 intact catalytic-site activity is needed in order to observe the morphogenic changes of GP135 staining.

PtdIns(3,4)P2, the SHIP2 product at the basolateral membrane, can bind to Dlg1

Par3/Par6/atypical protein kinase C, Scribble/Lgl/Dlg, and Crumbs/Stardust/PATJ complexes are important regulators of apicobasal polarization (Wodarz, 2002). Par3 is targeted to the plasma membrane by direct binding

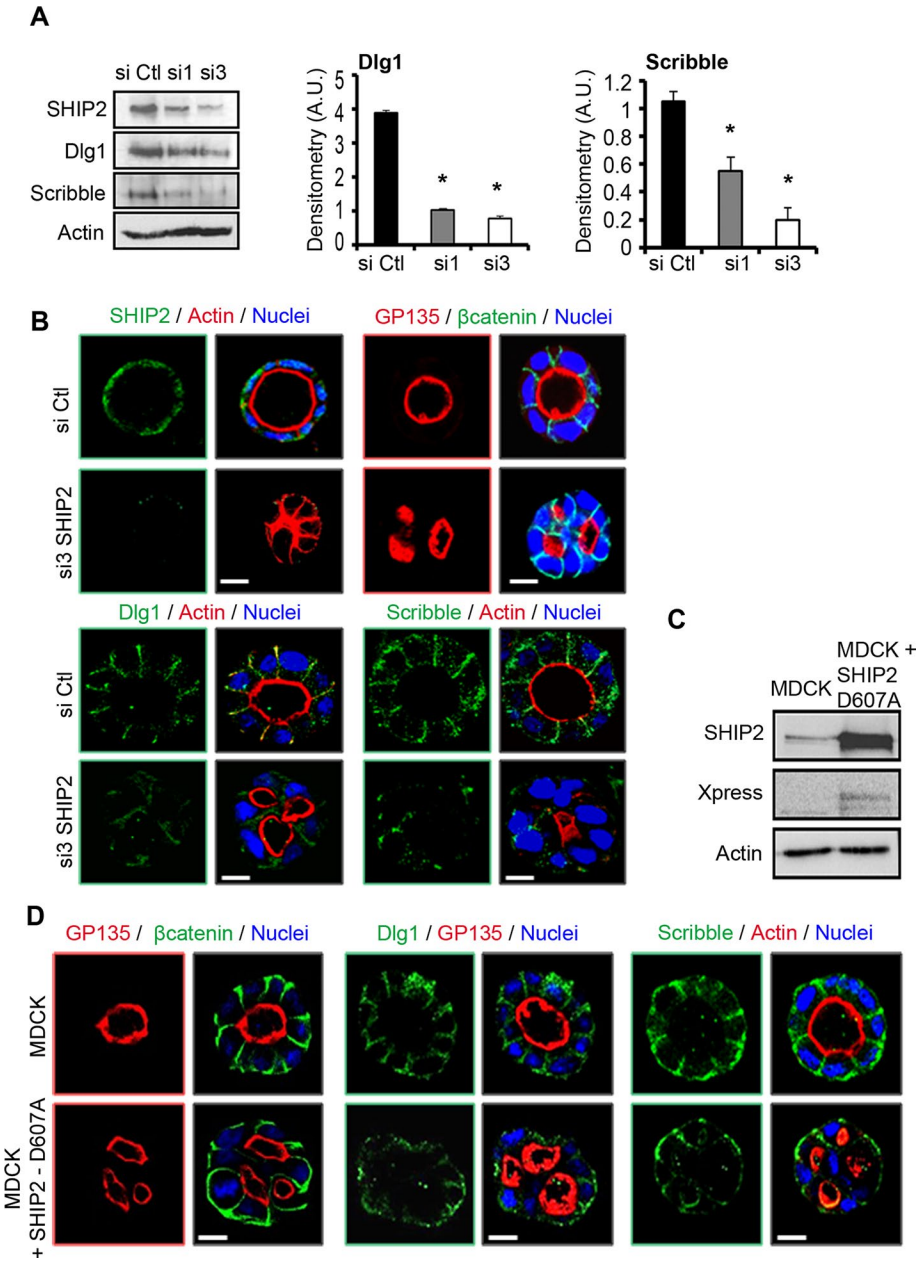

FIGURE 4: Depletion of SHIP2 or inhibition of its catalytic activity disrupts cell polarity. (A) Immunoblot analysis of SHIP2, Dlg1, and Scribble in cells treated with two different SHIP2-specific siRNAs (si1 and si3). Actin is used as loading control. Densitometry analysis normalized to actin from three independent experiments is represented in arbitrary units (A.U.) in histograms. Error bars, SD. *$p < 0.05$. (B) MDCK cells transfected or not (si Ctl) with SHIP2 siRNA (si3) grown in Matrigel for 4 d to form cysts and stained for SHIP2, β-catenin, Dlg1, or Scribble (green) and actin or GP135 (red) as indicated. Nuclei (blue) were stained with TO-PRO-3. Single confocal section through the middle of cyst. Scale bar, 10 μm. (C) Immunoblot analysis of SHIP2 in MDCK cells transfected or not (MDCK) with the cDNA of SHIP2 phosphatase-dead mutant (SHIP2-D607A). Xpress antibody was used to detect expressed tagged SHIP2. Actin is used as loading control. (D) The cells treated as in C grown in Matrigel for 4 d to form cysts and stained for β-catenin, Dlg1, or Scribble (green) and actin or GP135 (red) as indicated. Nuclei (blue) were stained with Hoechst. Single confocal section through the middle of a cyst. Scale bar, 10 μm.

to phosphoinositides via its PSD-95/Discs large/zonula-occludens-1 (PDZ) domain (Krahn *et al.*, 2010). On the basis of these reports and our data (Figure 4), we hypothesized potential binding of PtdIns(3,4)P2, the lipid product of SHIP2, to Scribble and Dlg1.

First we confirmed that SHIP2 is responsible for the production of PtdIns(3,4P)2 at the basal membrane. MDCK cells were transfected with Xpress-tagged SHIP2 or the catalytic mutant of SHIP2 (D607A) cDNAs and grown in 3D on Matrigel to form cysts. The efficiency of the transfection was evaluated by immunoblot using either the SHIP2 or the Xpress antibodies (Figure 5A). The transfection led to an increase in SHIP2 expression at the basal membrane compared with control MDCK cells, accompanied by enrichment of PtdIns(3,4)P2 at the basal membrane (Figure 5B, middle). In contrast, the PtdIns(3,4)P2 signal was strongly reduced and dispersed in cysts expressing the catalytic mutant of SHIP2 (D607A) (Figure 5B, bottom). Thus these data argue in favor of the presence of PtdIns(3,4)P2 at the basal membrane and its production by SHIP2.

Next we performed a PIP-Strip overlay assay using lysates from polarized MDCK cells and probed the strip with Dlg1 and Scribble antibodies. The data show that Dlg1 bound mainly to PtdIns(3,4)P2 and to a lesser extent PtdIns(3,4,5)P3 (Figure 5C). No signal was observed for Scribble (data not shown). To quantify the relative affinity, we next performed a PIP array and spotted each lipid in seven different concentrations (Figure 5D). Although there is low binding to other PtdIns species, here again PtdIns(3,4)P2 appeared as the preferential ligand for Dlg1 and could be responsible for its membrane localization.

Overexpression of SHIP2 and not the catalytic-inactive mutant rescues polarity and restricts HCV core expression

On the basis of the negative regulation of SHIP2 and its lipid product, PtdIns(3,4)P2, by HCV, and given the apparent similarity between the cellular effects of HCV core and SHIP2 depletion, we hypothesized that SHIP2 is a cellular target for HCV to disrupt polarity. To confirm this hypothesis, we transfected Xpress-tagged SHIP2 in MDCK core cells (Figure 6). The cell lysates were analyzed by immunoblotting using both SHIP2 and Xpress antibodies, and data indicated the efficiency of the transfection (Figure 6B). We also observed a slight but nonsignificant decrease of core protein in SHIP2-transfected cells (Figure 6C). Cells transfected with 2 μg of cDNA were grown on Matrigel to form cysts and analyzed by confocal microscopy (Figure 6A). The staining of cysts with SHIP2 and actin confirmed the reduction of SHIP2 expression at basal levels in core-induced multilumen cysts, as observed in Figure 3A. Strikingly, expression of SHIP2 visualized by both SHIP2 (Figure 6A,

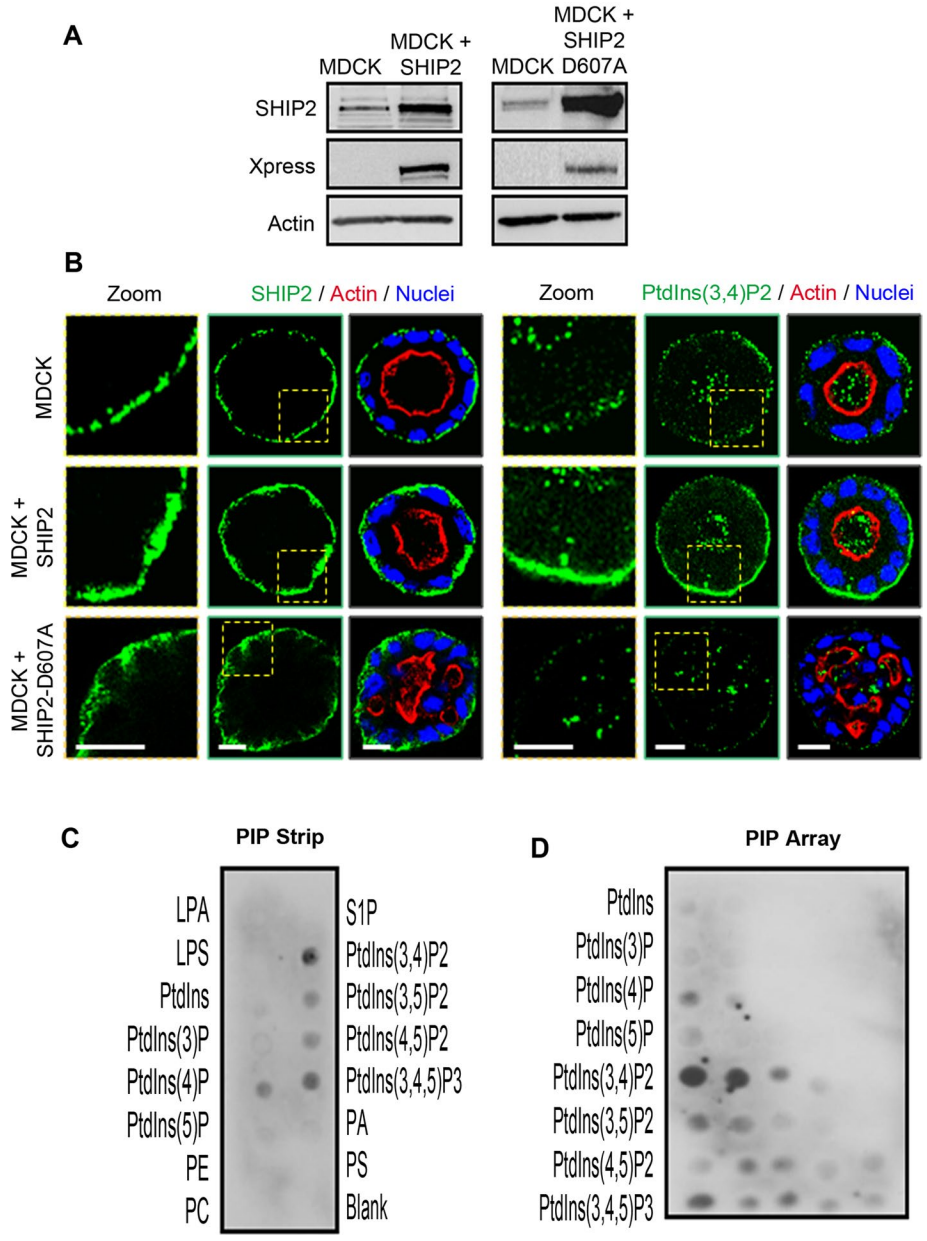

FIGURE 5: SHIP2 produces PtdIns(3,4)P2, which binds to dlg1. (A) Immunoblot analysis of SHIP2 in MDCK cells transfected or not with cDNA SHIP2 or SHIP2 phosphatase-dead mutant (SHIP2-D607A). Xpress served to detect exogenous tagged SHIP2, and actin was used as loading control. (B) MDCK cells transfected or not (MDCK) with cDNA SHIP2 or SHIP2 phosphatase-dead mutant (SHIP2-D607A) grown in Matrigel for 4 d to form cysts and stained for SHIP2 or PtdIns(3,4)P2 (green) and actin (red) as indicated. Nuclei (blue) were stained with Hoechst. Single confocal section through the middle of a cyst. Left, a zoom. Scale bar, 10 μm. (C) PIP-Strips or (D) PIP array with the indicated immobilized phospholipids incubated with homogenates from MDCK cells grown for 48 h on culture dishes. Bound proteins were detected using anti-Dlg1 antibody followed by secondary antibody and luminescence detection as described in *Materials and Methods*.

left) and Xpress (Figure 6A, middle) antibodies was sufficient to rescue the polarized phenotype, and cysts recovered a single lumen, as indicated by actin staining. Data from analysis of ~200 cysts indicated that 67% of the cysts presented both normal lumen and Xpress expression (Figure 6D). Although immunoblot analysis did not reveal a significant reduction of core expression in the lysates of SHIP2-transfected cells (Figure 6B), a significant decrease of core signal was observed in the cysts that recovered a single lumen (Figure 6A, right). Thus we chose to further evaluate by immunostaining the coexpression and localization of core and SHIP2 (Figure 6E). In MDCK core cysts, as expected, core is highly expressed and present at the cell membrane in contact with ECM, whereas SHIP2 expression is very weak (Figure 6E, left). The opposite data were observed when SHIP2 was reexpressed. These results were highlighted by the 3D reconstruction of the different confocal sections of cysts. These pictures clearly show the recovery of the spherical structure of cysts in the presence of SHIP2. The staining of both SHIP2 and core was quantified using ImageJ software and is presented below the pictures as histograms (Figure 6E). Furthermore, cells were transfected with SHIP2 phosphatase dead mutant to determine its effect on cell polarization. The transfection efficiency was validated by immunoblot (Supplemental Figure S6A), and in such conditions, the mutant was not able to rescue polarity defects induced by HCV core, and even a slight increase of multilumen cysts was observed. Moreover, these cysts presented an increase number of lumens (Supplemental Figure S6B), underlining the importance of SHIP2 enzymatic activity to build polarity. Together these data revealed that SHIP2 is a gatekeeper of cell polarity and its presence at ECM–cell contact restricts HCV core expression.

Dlg1 depletion induces multilumen cyst formation but does not affect SHIP2 and scribble expression

Dlg1 belongs to the key polarity complexes, which are evolutionarily conserved from simple organisms to humans. Our data indicate an interaction between Dlg1 and the lipid product of SHIP2, and treatment of cells with SHIP2 siRNA induces a significant decrease of Dlg1. Moreover, Dlg1 expression is reduced in core-containing cells. On this basis, we analyzed the phenotype of Dlg1 depletion in MDCK using three specific siRNAs. Immunoblot analysis indicated that the three siRNAs efficiently reduced Dlg1 expression, and in such conditions no significant change was observed in SHIP2 expression (Figure 7A). By contrast, Figure 4 shows a significant decrease of Dlg1 expression in MDCK cells treated with SHIP2 siRNA, suggesting that SHIP2 acts upstream of Dlg1, and no feedback was observed. No change also was observed for Scribble expression, a known partner of Dlg1 in adherent junctions. Dlg1 knockdown led to the formation of filled lumens and multilumen cysts representing respectively 13 and 52% of 430 cysts counted from three experiments with si3 (Figure 7B). Figure 7C shows the number of polarized cysts remaining after treatment with the three

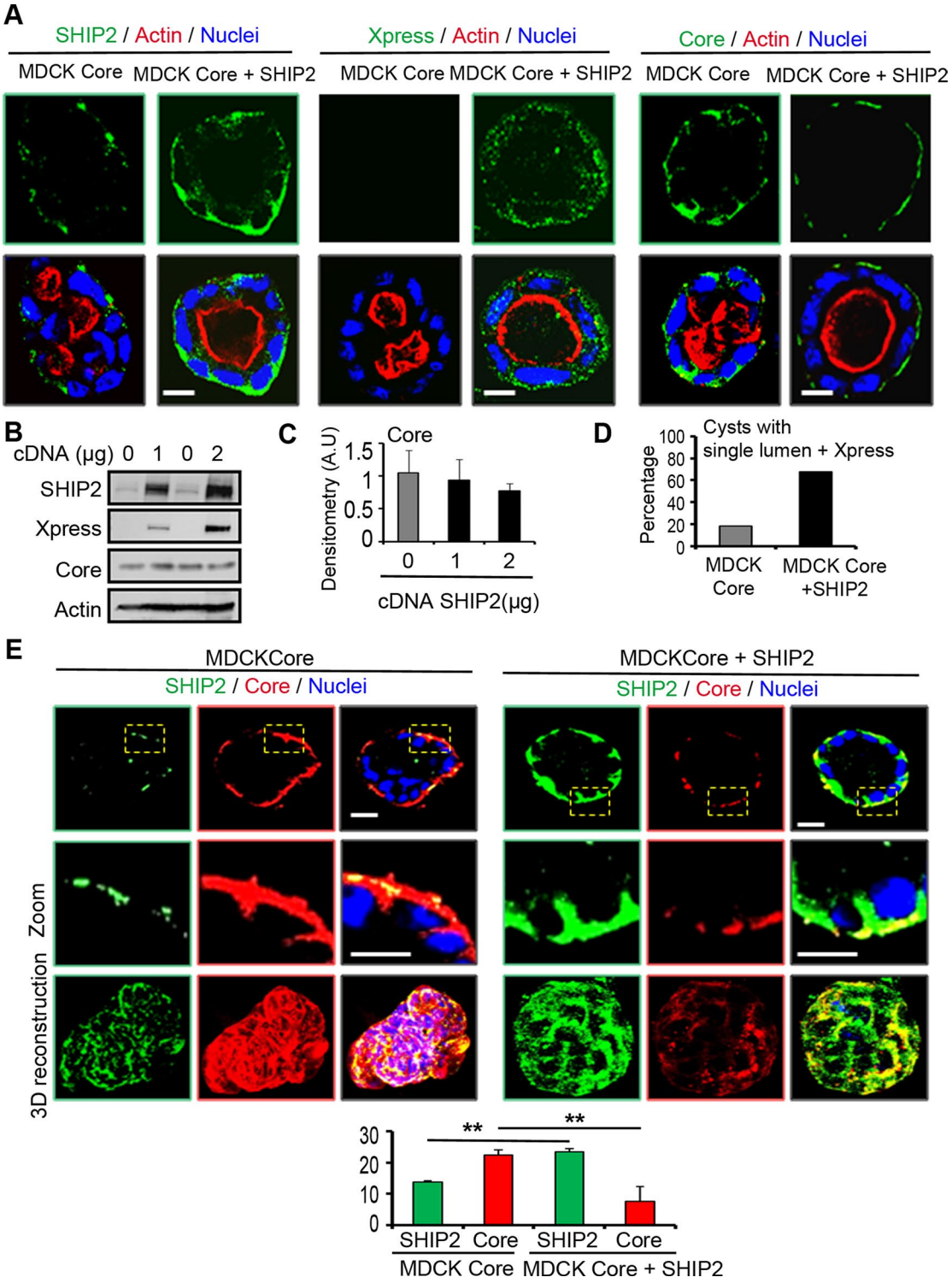

FIGURE 6: SHIP2 rescues polarity and negatively controls core protein expression in MDCK core cells. (A) MDCK core transfected or not with 2 µg of Xpress-tagged SHIP2 cDNA grown for 4 d in Matrigel and stained for SHIP2, Xpress, or Core (green) and actin (red) as indicated. Nuclei were stained with Hoechst (blue). Single confocal section through the middle of a cyst. Scale bar, 10 µm. (B) MDCK core transfected or not with 1 or 2 µg of cDNA of SHIP2 was collected for analysis by Western blotting with SHIP2, core, and Xpress antibodies. Actin served as loading control. Core densitometry analysis normalized to actin of three independent experiments is represented in arbitrary units (A.U.) in histogram (C). Data are means, and error bars are SD. (D) Approximately 200 cells in A were counted. The percentage of polarized cysts with normal single lumen stained with actin and presenting also Xpress expression is represented in histogram. (E) Cells in A were stained for SHIP2 (green) and core (red) as indicated. Nuclei were stained with Hoechst (blue). Single confocal section through the middle of a cyst. Middle, a zoom. Scale bar, 10 µm. Bottom, 3D reconstruction. The staining intensity of Core and SHIP2 were quantified with ImageJ from 15 cysts in three independent experiments and is presented in histograms. Error bars, SD. $^{**}p < 0.001$.

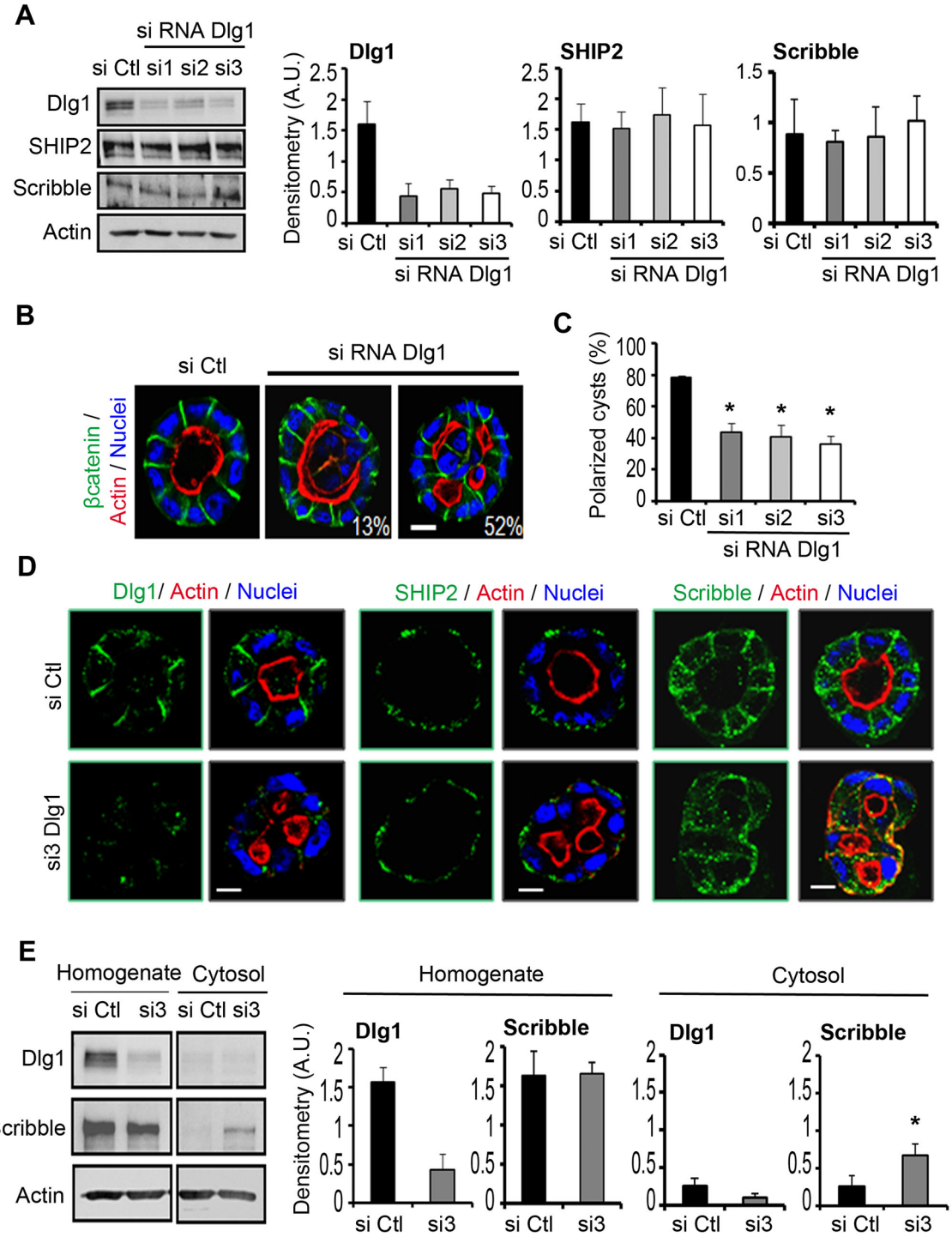

FIGURE 7: Dlg1 depleted cells form multilumen cysts. (A) MDCK cells transfected or not (si Ctl) with siRNA from Dlg1 (si1, si2, and si3) were grown for 3 d and cell lysates analyzed by immunoblotting with Dlg1, SHIP2, Scribble, and actin antibodies. The densitometry analysis from three independent experiments normalized to actin is represented in arbitrary units (A.U.) in histograms. Error bars, SD. *$p < 0.05$. (B) Cells transfected or not with si3 Dlg1 were grown for 4 d in Matrigel and stained for β-catenin (green) and actin (red) as indicated. Nuclei were stained with Hoechst (blue). Single confocal section through the middle of a cyst. Scale bar, 10 μm. Approximately 200 cells were counted from three independent experiments. The percentage of lumen-filled cysts and multilumen cysts is indicated. (C) Cells in A were grown for 4 d in Matrigel, and ~200 cells were counted from three independent experiments. The percentage of polarized cysts with normal single lumen is represented in the histogram. Error bars, SD. *$p < 0.05$. (D) Cells treated as in B stained for Dlg1, Scribble, or SHIP2 (green) and actin (red) as indicated. Nuclei were stained with Hoechst (blue). Single confocal section through the middle of a cyst. Scale bar, 10 μm. (E) Homogenates from MDCK cells transfected or not with si3 Dlg1 were submitted to ultracentrifugation at 100,000 × *g* into separate cytosolic compartments and immunoblotted for Scribble and Actin as loading control. Densitometry analysis normalized to actin from three independent experiments is represented in arbitrary units (A.U.) in histograms. Error bars, SD. *$p < 0.05$.

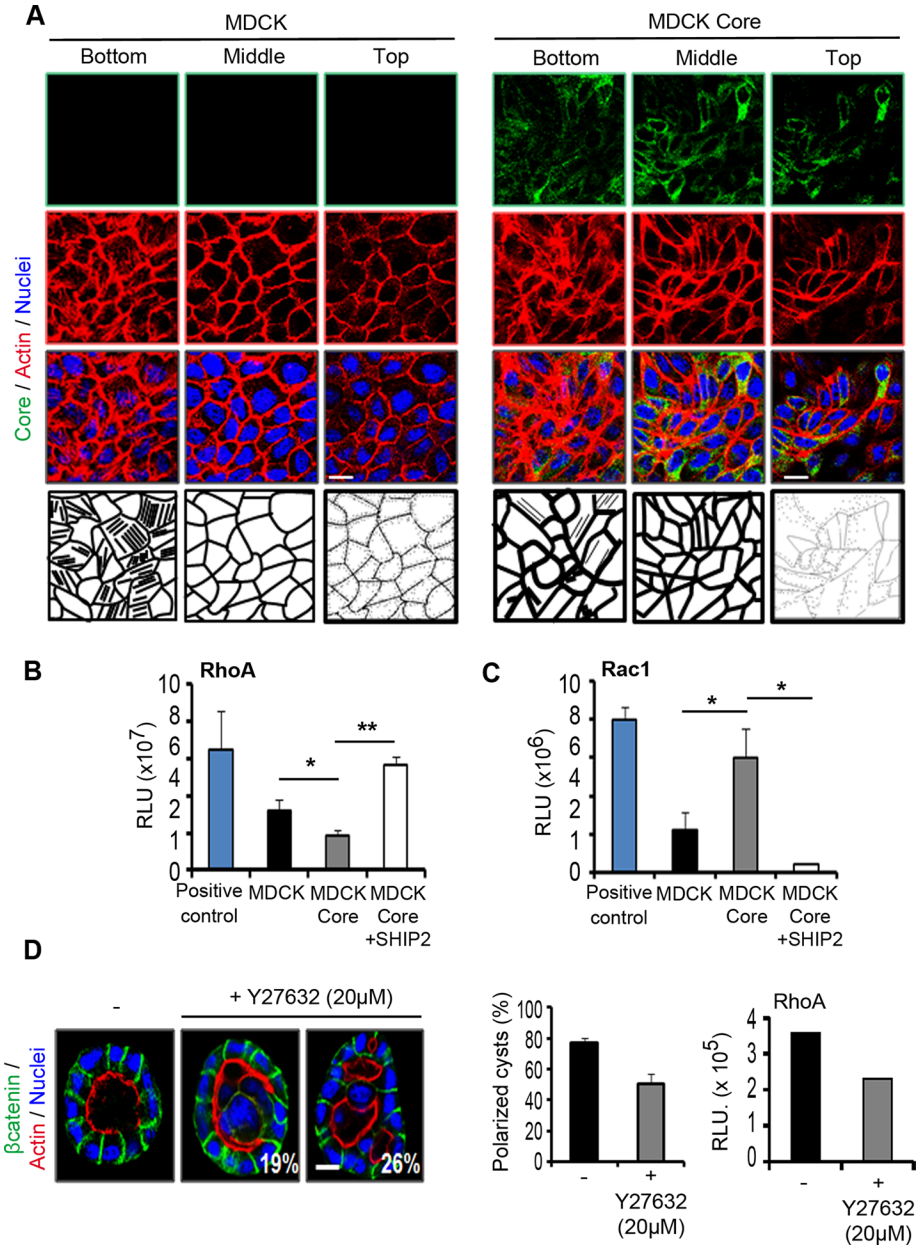

FIGURE 8: HCV core affects actin organization and Rho-family GTPases activities. (A) MDCK cells expressing or not HCV core protein were grown for 3 d on coverslips and stained for core (green) and actin (red) as indicated. Nuclei (blue) were stained with Hoechst. Three confocal images are shown, at the bottom, middle, and top of the cell. Scale bar, 10 μm. Bottom, schematic image. (B) Extracts from MDCK core cells transfected or not with SHIP2 cDNA were used to quantify RhoA and Rac1 (C) activation using G-LISA Biochem Kit (luminescence based). Intensity was measured by luminometer at 0.3 s. Negative control intensity was reduced from sample intensity, as indicated in the protocol. RLU, relative light unit. Error bars, SD. *$p < 0.05$, **$p < 0.001$. (D) MDCK cells were grown on Matrigel, treated 24 h after plating with ROCK inhibitor Y27632 (20 μM) for 72 h, and fixed and stained for β-catenin (green) and actin (red) as indicated. Nuclei (blue) were stained with Hoechst. Scale bar, 10 μm. We counted 150 cysts from two independent experiments. Percentage of lumen-filled and multilumen cysts is indicated. The percentage of polarized cysts with normal single lumen is represented in the histogram. Error bars, SD. Cells in D were used to quantify RhoA activation as in B.

different siRNAs. Furthermore, Dlg1-depleted cysts were analyzed by confocal microscopy for Scribble and SHIP2, and data indicated some staining of scribble in the cytoplasm (Figure 7D). Consequently we performed subcellular fractionation using ultracentrifugation, and immunoblot data indicated that Scribble is enriched in the cytosol of cells treated with Dlg1 siRNA compared with control cells (Figure 7E), strongly suggesting that Dlg1 expression regulates Scribble cellular localization.

HCV core cellular expression affects focal contacts, actin organization, and Rho-family GTPase activities

Cell–cell and cell–ECM adhesions provide essential cues to organize the apicobasal axis for polarization in epithelial cells. These spatial cues, mediated by integrins, induce cytoskeleton assemblies to serve as scaffolds for recruitment and binding of signaling molecules such as talin and paxillin. These events are important for stabilizing cell adhesion and regulate cell shape and polarity (Boudreau and Jones, 1999; Nelson, 2003; Bryant and Mostov, 2008). Thus the presence of HCV core protein at the membrane in contact with ECM led us to examine its effects on both paxillin and actin organization. In MDCK core cysts there is no significant change in paxillin expression compared with control cells, whereas the level of phosphorylated paxillin significantly increased in the presence of core (Supplemental Figure S7A) and was enriched at the cyst periphery, as shown by confocal microscopy (Supplemental Figure S7B).

Paxillin binds to many proteins involved in the organization of actin cytoskeleton required for many biological processes, including cell migration and polarization (Brown and Turner, 2004). Indeed we observed a change in actin organization forming the multilumen phenotype in 3D systems and decided to further examine this change using cells grown on cover glasses (Figure 8A). In control MDCK cells, actin stress fibers were visible and well organized in the bottom part of the culture, as indicated in the figure. In MDCK core cells, however, stronger actin cables were observed (Figure 8A).

The Rho family of GTPases are the master regulators of actin cytoskeleton remodeling, particularly RhoA and Rac1, which regulate the formation of stress fibers and lamellipodia, respectively (Burridge and Wennerberg, 2004) and play a pivotal role in cell polarity (O'Brien *et al.*, 2001; Yu *et al.*, 2008). Thus we decided to measure both RhoA and Rac1 activation in the presence of HCV core protein. Consistent with the change of stress fibers observed in MDCK core cells (Figure 8A), RhoA activation was significantly reduced in these cells compared with control MDCK cells (Figure 8B). Of interest, transfection of MDCK core cells with SHIP2 was associated with a significant increase of RhoA activation (Figure 8B). The opposite effects were observed for Rac1 assay (Figure 8C) and indicated that HCV core activates Rac1 and disrupts

cell adhesion to induce reorganization of actin cytoskeleton and loss of cell polarity. Consistent with these data, treatment of MDCK cells with the Rho-associated protein kinase (ROCK) inhibitor Y27632 induced the formation multilumen cysts, as observed with SHIP2 siRNA and HCV core cysts. Moreover, as observed using Dlg1 siRNA (Figure 7B), lumen-filled cysts were also formed (Figure 8D). Figure 8E shows the reduction of RhoA activation in the presence of Y27632.

DISCUSSION

This study illustrates a new mechanism for HCV core to disrupt cell polarity by subverting PI(3,4)P2 metabolism. HCV core protein plays an important role in HCV replication and also affects various intracellular signal events in its host, as well as changes in cell morphogenesis (Kunkel and Watowich, 2004; Boulant *et al.*, 2008; Jones and McLauchlan, 2010). Besides the liver tropism of HCV, studies with different cell lines such as HeLa and Caco-2 cells have contributed to understanding fundamental mechanisms regulating the close association of the HCV life cycle to host cellular functions (Kanda *et al.*, 2007; Mee *et al.*, 2008; Icard *et al.*, 2009).

Here we used MDCK cells grown in three dimensions as a model system to analyze the connection between HCV core protein and epithelial cell apicobasal polarity. The report of localization of HCV core protein at cell–ECM contacts in polarized epithelial cells is unprecedented. This localization was observed in both Huh7 and MDCK cells grown on filters and was underlined in MDCK grown in three dimensions. HCV core–induced loss of polarity and cysts presented a multilumen phenotype, accompanied by significant reduction of SHIP2 expression and its lipid product, PtdIns(3,4)P2.

Both SHIP2 and PtdIns(3,4)P2 are localized at cell–ECM contacts and critical to maintain apicobasal polarity. In earlier reports we showed that PTEN and its lipid product, PtdIns(4,5)P2, are concentrated at the apical membrane, where PtdIns(3,4,5)P3 and PI3K are mostly at the basolateral membrane (Gassama-Diagne *et al.*, 2006; Martin-Belmonte *et al.*, 2007). This work showed the presence of both SHIP2 and its lipid product, PtdIns(3,4)P2, at the basolateral membrane, indicating that the two major phosphatases that degrade PtdIns(3,4,5)P3, SHIP2 and PTEN, have opposite localizations in polarized epithelial cells. Similarly, chemotaxing neutrophils require SHIP1 for polarization at the leading edge (Nishio *et al.*, 2007), whereas PTEN was previously described at the uropod (Phillipson and Kubes, 2011). A recent report indicated the importance of SHIP2 in polarization and migration of glioma cells (Kato *et al.*, 2012). These data using migrating cells underscore our results in epithelial cell polarization, and we confirm here that SHIP2 is an effector of RhoA as depicted in Figure 8.

PTEN regulated the apical recruitment of Par3, Par 6, and cdc42, and, of interest, Par 3 membrane targeting depends on the binding of its PDZ domain to PtdIns(4,5)P2, the product of PTEN (Wu *et al.*, 2007; Krahn *et al.*, 2010). These data suggest that the lipid product of PTEN is critical for recruitment of polarity proteins. Similarly, we showed that the SHIP2 active site is required to maintain basolateral polarity. Moreover, our data indicate that Dlg1 binds to PI(3,4)P2 and thus could serve as scaffold to recruit other proteins at the membrane (e.g., Scribble), and underlining the role of the SHIP2 lipid product at the basolateral membrane. Of interest, depletion of Dlg1 led to Scribble cytoplasmic localization and strongly suggested the important role of Dlg1 in the stabilization of the polarity protein complex at the basolateral domain. However, more studies are required using purified proteins to make precise the eventual partners and the domain of Dlg1 protein involved in its binding to PtdIns(3,4)P2.

The multi–PDZ domain protein FRMPD2 is a potential scaffolding protein consisting of an N-terminal KIND domain, a FERM domain, and three PDZ domains. A previous report showed that FRMPD2 is localized in a polarized manner in epithelial cells at the basolateral membrane. The binding of FRMPD2 to PtdIns(3,4P)2 depends on its PDZ2 domains and is sufficient for its basolateral localization (Stenzel *et al.*, 2009), strongly suggesting that the same mechanism, governed by the specific interaction of the PDZ domain of the polarity proteins to PtdInsP, could be responsible for polarization in epithelial cells.

Our demonstration that SHIP2 is mainly located at the cell–ECM contact in polarized cells (Figure 3A) may be also related to different reports on SHIP2's role as a docking protein for a large number of cytoskeletal and focal adhesion proteins and tyrosine kinase–associated receptors (Dyson *et al.*, 2001; Prasad *et al.*, 2001; Paternotte *et al.*, 2005; Xie *et al.*, 2008; Zwaenepoel *et al.*, 2010; Erneux *et al.*, 2011; Elong Edimo *et al.*, 2013). Accordingly, we suggested that SHIP2 could regulate polarity by the stabilization of both cell–cell and cell–ECM contacts as illustrated in the model Figure 9.

Similar to HCV core, loss of SHIP2 or expression of a phosphatase-dead mutant in MDCK cells led to the formation of multilumen cysts. Overexpression of SHIP2 in MDCK cells rescued cell polarity and restricted the presence of core at cell–ECM contacts, indicating that core exhibits mutual antagonism with SHIP2 for localization at the basal membrane. In this context we showed that HCV core disorganized focal contacts and increased paxillin phosphorylation at tyrosine 118. This may induce loss of adhesion properties and rigid actin cortex to create a more dynamic cytoskeleton and promote spreading, lamellipodia formation, and cell migration, driven by Rac1. These data emphasize the involvement of HCV core in processes that lead to loss of cell adhesion and polarization. Earlier studies described the contribution of HCV core to epithelial-to-mesenchymal transition driven by tumor growth factor β signaling, although cellular localization of core protein was not analyzed (Battaglia *et al.*, 2009).

HCV is a one of the major causes of chronic hepatitis, which can result in cirrhosis and hepatocellular carcinoma (Rice, 2011). Disturbed polarization is a hallmark of cancer, and thus HCV might be able to highjack the polarity mechanisms dependent on SHIP2 to invade and spread in the host cell, leading to loss of polarity and development of carcinogenesis. Nevertheless, although the antitumor activity of PTEN is dogma, data concerning SHIP2 are contradictory. SHIP2 down-regulation is described in hepatocarcinoma samples from patients infected with HCV (Sumie *et al.*, 2007) and, intriguingly, elevated expression of SHIP2 was described in several primary breast cancer cells (Prasad *et al.*, 2008). These discrepancies could be due to both tissue and cancer origin, and thus the link between SHIP2 and cancer development needs further research.

To conclude, we illustrate a critical role of SHIP2 in apicobasal polarity of epithelial cells, increasing our understanding of the role of phosphoinositides, particularly PI(3,4)P2, in cell polarization. This highlights the usefulness of studies on the interaction between pathogens and their host cells to address fundamental questions of cell biology (Rodriguez-Boulan *et al.*, 1983; Mellman and Nelson, 2008; Cossart, 2011). A report implicated SHIP2 in the dissemination of vaccinia virus, another enveloped virus whose life cycle is regulated by lipid metabolism (McNulty *et al.*, 2011), suggesting a larger usurpation of SHIP2 signaling by enveloped virus beyond HCV. This work pointed out the contribution of SHIP2 and its partners (Dlg1, RhoA) as new cellular targets for research against virus infection.

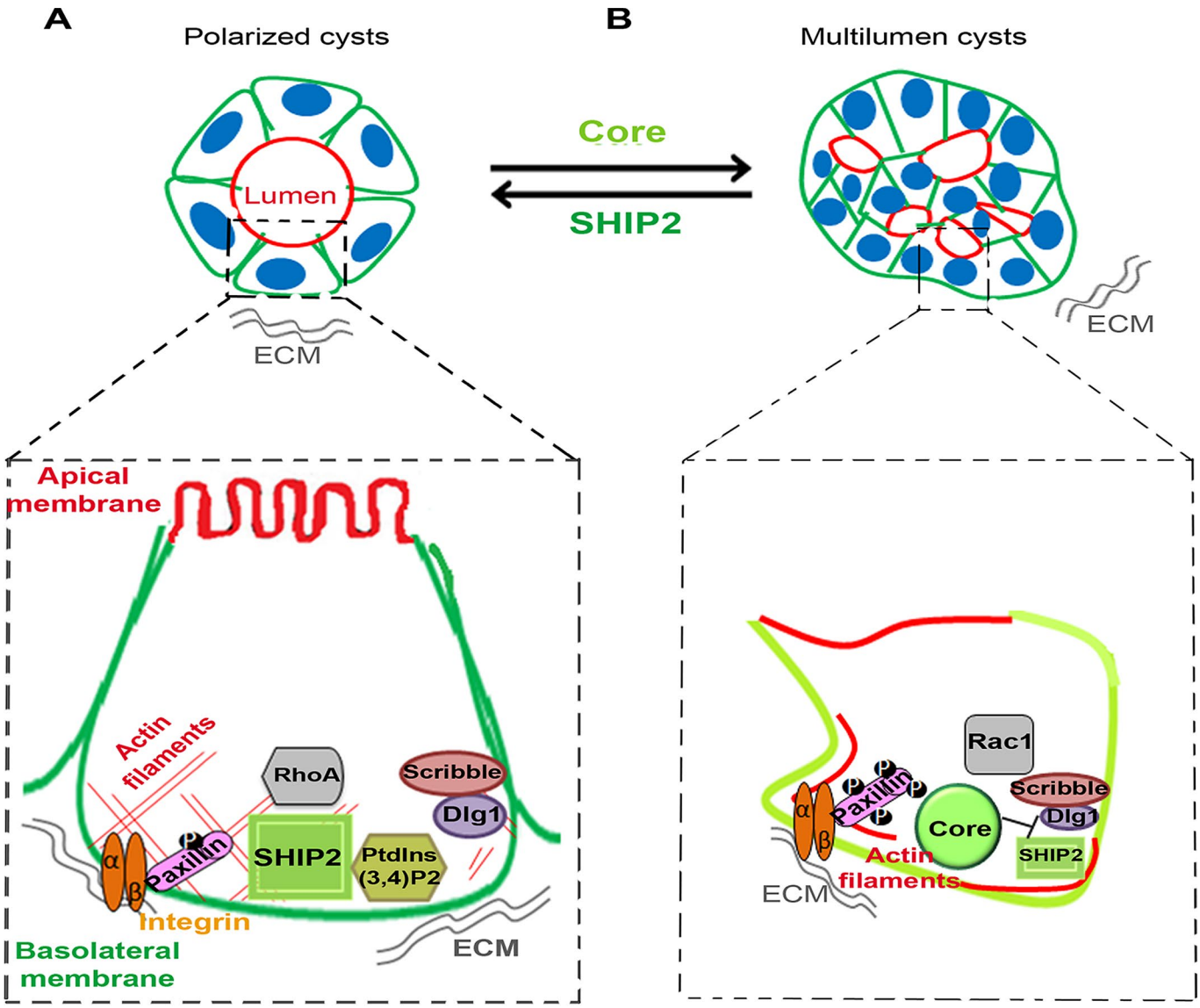

FIGURE 9: Schematic model of polarized cell and loss of polarity induced by the HCV core. (A) Polarized MDCK cyst showing an apical membrane toward the lumen and a basolateral membrane in contact with the extracellular matrix (ECM). A zoom is presented to illustrate SHIP2 at the basal membrane, underlining its enzymatic activity to produce PtdIns(3,4)P2 at the basolateral membrane and its role in cell polarity by activating RhoA, inducing stabilization of both cell–cell (Dlg1-Scribble) and cell–ECM (paxillin) contacts. (B) Multilumen cyst presenting the phenotype of cells expressing HCV core protein. A zoom is presented to illustrate the loss of cell polarity in cells expressing HCV core protein, indicating mutual antagonism between SHIP2 and core for localization at the basal membrane. Disorganization of focal contacts and increase of paxillin phosphorylation at tyrosine 118 and Rac1activity are also seen.

MATERIALS AND METHODS

Reagents

Anti-actin (mouse) was from Sigma-Aldrich (St. Louis, MO), anti–β-catenin, Dlg1 (rabbit), anti-SHIP2 (goat and rabbit), and anti-Scribble (goat) were from Santa Cruz Biotechnology (Santa Cruz, CA); anti-PtdIns(3,4)P2 was from Echelon (Salt Lake City, UT); anti-paxillin, phosphopaxillin (Cell Signaling Technology, Danvers, MA), and core antibodies were from Abcam (Cambridge, MA). Mouse anti-GP135 was a gift from George Ojakian (SUNY Downstate Medical Center, Brooklyn, NY). Anti-Par3 was from Millipore (Billerica, MA), and rat anti-ZO-1 antibody was a gift from Bruce Stevenson (University of Alberta, Edmonton, AB, Canada). E-cadherin was from BD Biosciences (San Diego, CA), and anti-Xpress was from Invitrogen (Carlsbad, CA). Secondary antibodies used were highly cross-absorbed anti-mouse Alexa Fluor 546 and anti-rabbit Alexa Fluor 488 (Invitrogen), goat anti-rabbit or anti-mouse horseradish peroxidase (HRP), and anti-goat HRP (Sigma-Aldrich). Actin and nuclei were stained respectively with Alexa Fluor 546 phalloidin and Hoechst (both from Invitrogen).

Construction of stable cell lines

Full-length HCV core sequences were amplified by PCR from RNA extracted from tumor of a patient infected with HCV 1b genotype and cloned into the pcDNA3.1 vector as previously described (Pavio *et al.*, 2005).

The Huh7 cells were transfected with a construction using the Lipofectamine method (Invitrogen), and stable transfectants were selected by incubating cells with Geneticin (Battaglia *et al.*, 2009). The same procedure was used for MDCK stable transfectants.

Cell culture

MDCK and MDCK containing HCV core cells were maintained in MEM containing Earle's balanced salt solution supplemented with 5% fetal bovine serum and 1% penicillin/streptomycin solution (10,000 U/ml, 10,000 µg/ml) at 37°C in 5% CO_2, 95% air. For two-dimensional culture, MDCK cells were grown as monolayer on Transwell filters (Corning, Tewksbury, MA). Culture medium was added over and under the filter and changed after 48 h. Cells were grown for 3 d.

The 3D culture of MDCK cells in Matrigel was performed as described previously for MCF10A cells (Martin-Belmonte *et al.*, 2007). In brief, MDCK cells were trypsinized as a single-cell suspension of 2×10^4 cells/ml in 2% Matrigel (BD Biosciences) and 500 µl of cells was plated in each well of eight-well Lab-Tek II chamber slides (Thermo Fisher Scientific, Waltham, MA) precovered with Matrigel and covered with a 1- to 2-mm-thick solidified layer of 100% Matrigel. Cells were fed every 2 d and grown for 4–5 d until cysts with lumen formed. For drug treatment, 20 mM Y27632 (ROCK inhibitor; Sigma-Aldrich) was added 24 h after cell plating.

Huh7 or Huh7 containing HCV core (Huh7 core) cells were cultured in DMEM containing 4.5 g/l glucose supplemented with 10% heat-inactivated fetal bovine serum, 1% nonessential amino acids, and 1% penicillin/streptomycin and Geneticin (G418; Sigma-Aldrich).

Cell transfection

siRNA. The specific SHIP2 duplex RNA interference (RNAi) used was 5′GGUCAAUUGCCGAGAUUAC3′ and 5′GCUAUACGUAAGGCCAAGA3′ (Sigma-Aldrich).

The Dlg1 duplex RNAi used was 5′GAUAUCCUCCAUGUUAUUA3′ for si1, 5′GGAAUAUUUAUUUCCUUUA3′ for si2, and 5′CAACUCUUCUUCUCAGCCU3′ for si3 (Sigma-Aldrich).

cDNA. The wild-type human SHIP2 (SHIP2) and the catalytic-dead mutant SHIP2 (SHIP2 D607A) in pCDNA3 His vector were reported before (Pesesse *et al.*, 2001; Zhang *et al.*, 2007). The plasmid DNA was isolated using the Maxi-Prep plasmid purification Kit (Qiagen, Valencia, CA). The GFP-SHIP2 and YFP-TAPP were provided by Nicolas Leslie (University of Dundee, Dundee, Scotland, United Kingdom).

MDCK cells seeded at low density (10^4 cells/cm^2) were transfected with 20 nM solutions of specific RNAi or cDNA using Lipofectamine RNAi MAX Reagent (Invitrogen) or jetPRIME (Ozyme, Montigny-Le-Bretonneux, France) according to the manufacturer's instructions and incubated for 48 h. For 3D culture, 24 h after transfection, cells were detached with trypsin and plated on Matrigel for 4 d as indicated.

Immunolabeling

MDCK cells were rinsed with ice-cold Dulbecco's phosphate-buffered saline (DPBS) and fixed with 3.7% paraformaldehyde for 30 min. Samples were permeabilized and saturated with DPBS supplemented with 0.7% fish gelatin and 0.025% saponin for 30 min at 37°C and then incubated with primary antibodies. After washes, staining was performed with secondary fluorescent antibodies, phalloidin, and Hoechst or TO-PRO 3 (with previous RNase treatment). Samples were observed with a Zeiss 510 LSM confocal microscope (Carl Zeiss, Jena, Germany) or Leica TCS SP5 AOBS tandem microscope confocal (Leica, Wetzlar, Germany). Images were collected as TIF files and analyzed with Photoshop (Adobe, San Jose, CA) or Volocity software (PerkinElmer, Waltham, MA).

Cell fractionation

Cells were homogenized with Dounce in Tris (10 mM)/sucrose (250 mM) buffer, pH 7.4, containing protein and phosphatase inhibitors (Roche, Indianapolis, IN). The cell lysates were centrifuged at 1000 rpm for 10 min, and the supernatants were recentrifuged at 100,000 × *g* for 60 min. The membrane pellet and the supernatant (cytosol) were collected for protein quantification and analysis by immunoblot.

Immunoblot

The samples were harvested in Laemmli sample buffer and denatured at 100°C for 5 min before separation on 10% SDS–PAGE and then electrotransferred onto polyvinylidene fluoride membrane. After transfer, the membrane was saturated in DPBS containing 0.1% Tween 20 and 5% milk. Primary antibodies were added overnight at 4°C. After washes in the presence of DPBS, appropriate secondary antibodies coupled with peroxidase were added. Immunoblotting was revealed with chemiluminescent peroxidase substrate (Chemiluminescent Peroxidase Substrate-3; Sigma-Aldrich) and exposure on Biomax Light film (Kodak, Rochester, NY).

Protein-lipid overlay assay

Cells from confluent plates (10^5 cells/cm^2) were lysated in PBS containing protein and phosphatase inhibitor (Roche) and used for PIP-Strip or PIP array (Echelon) binding assays according to the manufacturer's protocol. First the strips were incubated for 1 h in 1% nonfat dry milk and then with cell lysates overnight at 4°C. After three washes, the membranes were incubated with primary anti-Dlg1 or Scribble antibodies overnight at 4°C and treated as described for immunoblotting.

Quantitative real-time PCR

Total RNA was isolated using RNeasy Mini Kit 50 (Qiagen) and applied to reverse transcription using RevertAid First Strand cDNA Synthesis Kit (Fermentas, Glen Burnie, MD). The cDNA was analyzed by quantitative PCR using Quanti Tect SYBR Green PCR Kit (Qiagen) with the 7500 Fast Real-Time PCR System (Applied Biosystems, Foster City, CA). Reaction parameters were 50°C for 30 min and 95°C for 15 min, followed by 45 cycles of 94°C for 15 s, 55°C for 30 s, and 72°C for 30 s. The triplicate mean values were calculated using glyceraldehyde-3-phosphate dehydrogenase gene transcription as reference for normalization.

The primers used for SHIP2 are forward, CTCAAGGAGCTCACAGATCTGG, and reverse, TGGCTGATTCGGTTCTCATGCT.

RhoA and Rac1 activation assay

RhoA and Rac1 activation was quantified using G-LIZA Biochem Kit (luminescence based) from tebu-bio (Le Perray-en-Yvelines, France) as described by the manufacturer. Briefly, cell lysates (1 µg/µl for protein concentration) were incubated in the affinity wells for 30 min at 4°C. Antigen presenting buffer was added for 2 min. Primary and secondary antibodies were incubated for 45 min at room temperature. Intensity was measured by luminometer at 0.3 s with HRP detection reagent. Cell lysis buffer was used as blank control, and RhoA or Rac1 control protein was used as positive control sample. Blanc control intensity was reduced from sample intensity, as indicated in the protocol.

Statistical analyses

Comparison of mean values was conducted with unpaired Student's *t* tests. Statistical significance was determined at $*p < 0.05$, $**p < 0.001$, and $***p < 0.0001$.

ACKNOWLEDGMENTS

We thank Christian Bréchot for useful critical discussions of the manuscript; Sophie Allart and Abdelali Jalil, imagery services at the Institut National de la Santé et de la Recherche Médicale Unité 563, Toulouse, and Institut Gustave Roussy, Villejuif, respectively; and Nassima Benzoubir and Marion Bourgeade, Institut National de la Santé et de la Recherche Médicale Unité 785, Villejuif, for providing the MDCK and Huh7 cell lines stably transfected with core. We thank Nicholas Leslie for providing the GFP-SHIP2 and YFP-TAPP constructs and for helpful discussions. This work was supported by grants from the Association pour la Recherche sur le Cancer (ARC/SUBV/CKLQ6) to A.G.D. and the Fonds de la Recherche Scientifique (Belgium) to C.E. We acknowledge the support of Pfizer to J.P.S. and the National Council for Scientific Research Lebanon for supporting A.A.

REFERENCES

Alvisi G, Madan V, Bartenschlager R (2011). Hepatitis C virus and host cell lipids: an intimate connection. RNA Biol 8, 258–269.

Backers K, Blero D, Paternotte N, Zhang J, Erneux C (2003). The termination of PI3K signalling by SHIP1 and SHIP2 inositol 5-phosphatases. Adv Enzyme Regul 43, 15–28.

Barba G *et al.* (1997). Hepatitis C virus core protein shows a cytoplasmic localization and associates to cellular lipid storage droplets. Proc Natl Acad Sci USA 94, 1200–1205.

Bartenschlager R, Penin F, Lohmann V, André P (2011). Assembly of infectious hepatitis C virus particles. Trends Microbiol 19, 95–103.

Battaglia S, Benzoubir N, Nobilet S, Charneau P, Samuel D, Zignego AL, Atfi A, Bréchot C, Bourgeade MF (2009). Liver cancer-derived hepatitis C virus core proteins shift TGF-beta responses from tumor suppression to epithelial-mesenchymal transition. PLoS One 4, e4355.

Benedicto I, Molina-Jiménez F, Barreiro O, Maldonado-Rodríguez A, Prieto J, Moreno-Otero R, Aldabe R, López-Cabrera M, Majano PL (2008). Hepatitis C virus envelope components alter localization of hepatocyte tight junction–associated proteins and promote occludin retention in the endoplasmic reticulum. Hepatology 48, 1044–1053.

Benedicto I, Molina-Jiménez F, Moreno-Otero R, López-Cabrera M, Majano PL (2011). Interplay among cellular polarization, lipoprotein metabolism and hepatitis C virus entry. World J Gastroenterol 17, 2683–2690.

Berger KL, Cooper JD, Heaton NS, Yoon R, Oakland TE, Jordan TX, Mateu G, Grakoui A, Randall G (2009). Roles for endocytic trafficking and phosphatidylinositol 4-kinase III alpha in hepatitis C virus replication. Proc Natl Acad Sci USA 106, 7577–7582.

Berger KL, Kelly SM, Jordan TX, Tartell MA, Randall G (2011). Hepatitis C virus stimulates the phosphatidylinositol 4-kinase III alpha-dependent phosphatidylinositol 4-phosphate production that is essential for its replication. J Virol 85, 8870–8883.

Bianco A *et al.* (2012). Metabolism of phosphatidylinositol 4-kinase IIIα-dependent PI4P Is subverted by HCV and is targeted by a 4-anilino quinazoline with antiviral activity. PLoS Pathog 8, e1002576.

Borawski J *et al.* (2009). Class III phosphatidylinositol 4-kinase alpha and beta are novel host factor regulators of hepatitis C virus replication. J Virol 83, 10058–10074.

Boudreau NJ, Jones PL (1999). Extracellular matrix and integrin signalling: the shape of things to come. Biochem J 339, 481–488.

Boulant S, Douglas MW, Moody L, Budkowska A, Targett-Adams P, McLauchlan J (2008). Hepatitis C virus core protein induces lipid droplet redistribution in a microtubule- and dynein-dependent manner. Traffic 9, 1268–1282.

Burridge K, Wennerberg K (2004). Rho and Rac take center stage. Cell 116, 167–179.

Brown MC, Turner CE (2004). Paxillin: adapting to change. Physiol Rev 84, 1315–1339.

Bryant DM, Mostov KE (2008). From cells to organs: building polarized tissue. Nat Rev Mol Cell Biol 9, 887–901.

Cantley LC (2002). The phosphoinositide 3-kinase pathway. Science 296, 1655–1657.

Comer FI, Parent CA (2007). Phosphoinositides specify polarity during epithelial organ development. Cell 128, 239–240.

Cossart P (2011). Illuminating the landscape of host-pathogen interactions with the bacterium *Listeria monocytogenes*. Proc Natl Acad Sci USA 108, 19484–19491.

Dyson JM, O'Malley CJ, Becanovic J, Munday AD, Berndt MC, Coghill ID, Nandurkar HH, Ooms LM, Mitchell CA (2001). The SH2-containing inositol polyphosphate 5-phosphatase, SHIP-2, binds filamin and regulates submembraneous actin. J Cell Biol 155, 1065–1079.

Erneux C, Edimo WE, Deneubourg L, Pirson I (2011). SHIP2 multiple functions: a balance between a negative control of PtdIns(3,4,5)P3 level, a positive control of PtdIns(3,4)P2 production, and intrinsic docking properties. J Cell Biochem 112, 2203–2209.

Elong Edimo W, Vanderwinden JM, Erneux C (2013). SHIP2 signalling at the plasma membrane, in the nucleus and at focal contacts. Adv Biol Regul 53, 28–37.

Gassama-Diagne A, Payrastre B (2009). Phosphoinositide signaling pathways: promising role as builders of epithelial cell polarity. Int Rev Cell Mol Biol 273, 313–343.

Gassama-Diagne A, Yu W, ter Beest M, Martin-Belmonte F, Kierbel A, Engel J, Mostov K (2006). Phosphatidylinositol-3,4,5-trisphosphate regulates the formation of the basolateral plasma membrane in epithelial cells. Nat Cell Biol 8, 963–970.

Herker E, Harris C, Hernandez C, Carpentier A, Kaehlcke K, Rosenberg AR, Farese RV Jr, Ott M (2010). Efficient hepatitis C virus particle formation requires diacylglycerol acyltransferase-1. Nat Med 16, 1295–1298.

Huber C *et al.* (2013). Exome sequencing identifies INPPL1 mutations as a cause of opsismodysplasia. Am J Hum Genet 92, 144–149.

Icard V, Diaz O, Scholtes C, Perrin-Cocon L, Ramière C, Bartenschlager R, Penin F, Lotteau V, André P (2009). Secretion of hepatitis C virus envelope glycoproteins depends on assembly of apolipoprotein B positive lipoproteins. PLoS One 4, e4233.

Jones DM, McLauchlan J (2010). Core is associated with different steps of HCV assembly. J Biol Chem 285, 22733–22739.

Kanda T, Yokosuka O, Mikata R, Zhang KY, Tanaka M, Tada M, Fukai K, Imazeki F, Saisho H (2007). Inhibition of subgenomic hepatitis C virus RNA replication in HeLa cells. Hepatogastroenterology 54, 32–35.

Kapadia SB, Chisari FV (2005). Hepatitis C virus RNA replication is regulated by host geranylgeranylation and fatty acids. Proc Natl Acad Sci USA 102, 2561–2566.

Kato K *et al.* (2012). The inositol 5-phosphataseSHIP2 is an effector of RhoA and is involved in cell polarity and migration. Mol Biol Cell 23, 2593–2604.

Kato T,, Date T, Miyamoto M, Zhao Z, Mizokami M, Wakita T (2005). Nonhepatic cell lines HeLa and 293 support efficient replication of the hepatitis C virus genotype 2a subgenomic replicon. J Virol 79, 592–596.

Kazmierczak BI, Mostov K, Engel JN (2001). Interactions of bacteria pathogens with polarized epithelium. Annu Rev Microbiol 55, 407–435.

Krahn MP, Klopfenstein DR, Fischer N,, Wodarz A (2010). Membrane targeting of Bazooka/PAR-3 is mediated by direct binding to phosphoinositide lipids. Curr Biol 20, 636–642.

Kunkel M, Watowich SJ (2004). Biophysical characterization of hepatitis C virus core protein: implications for interactions within the virus and host. FEBS Lett 557, 174–180.

Liu S, Yang W, Shen L, Turner JR, Coyne CB, Wang T (2009). Tight junction proteins claudin-1 and occludin control hepatitis virus entry and are downregulated during infection to prevent superinfection. J Virol 83, 2011–2014.

Marion E *et al.* (2002). The gene INPPL1, encoding the lipid phosphatase SHIP2, is a candidate for type 2 diabetes in rat and man. Diabetes 51, 2012–2017.

Martin S, Parton RG (2006). Lipid droplets: a unified view of a dynamic organelle. Nat Cell Biol 9, 1089–1097.

Martin-Belmonte F, Gassama A, Datta A, Yu W, Rescher U, Gerke V, Mostov K (2007). PTEN-mediated apical segregation of phosphoinositides controls epithelial morphogenesis through Cdc42. Cell 128, 383–397.

Mee CJ, Farquhar MJ, Harris HJ, Hu K, Ramma W, Ahmed A, Maurel P, Bicknell R, Balfe P, McKeating JA (2010). Hepatitis C virus infection reduces hepatocellular polarity in a vascular endothelial growth factor-dependent manner. Gastroenterology 138, 1134–1142.

Mee CJ, Grove J, Harris HJ, Hu K, Balfe P, McKeating JA (2008). Effect of cell polarization on hepatitis C virus entry. J Virol 82, 461–470.

Mee CJ, Harris HJ, Farquhar MJ, Wilson G, Reynolds G, Davis C, van IJzendoorn SC, Balfe P, McKeating JA (2009). Polarization restricts hepatitis C virus entry into HepG2 hepatoma cells. J Virol 83, 6211–6221.

McNulty S, Powell K, Erneux C, Kalman D (2011). The host phosphoinositide 5-phosphatase SHIP2 regulates dissemination of vaccinia virus. J Virol 85, 7402–7410.
Mellman I, Nelson WJ (2008). Coordinated protein sorting, targeting and distribution in polarized cells. Nat Rev Mol Cell Biol 9, 833–845.
Miyanari Y, Atsuzawa K, Usuda N, Watashi K, Hishiki T, Zayas M, Bartenschlager R, Wakita T, Hijikata M, Shimotohno K (2007). The lipid droplet is an important organelle for hepatitis C virus production. Nat Cell Biol 9, 1089–1097.
Moradpour D *et al.* (2007). Replication of hepatitis C virus. Nat Rev Microbiol 5, 453–463.
Moriya K, Yotsuyanagi H, Shintani Y, Fujie H, Ishibashi K, Matsuura Y, Miyamura T, Koike K (1997). Hepatitis C viruscore protein induces hepatic steatosis in transgenic mice. J Gen Virol 78, 1527–1531.
Moriya K *et al.* (2001). Oxidative stress in the absence of inflammation in a mouse model for hepatitis C virus-associated hepatocarcinogenesis. Cancer Res 61, 4365–4370.
Muthuswamy SK, Xue B (2012). Cell polarity as a regulator of cancer cell behavior plasticity. Annu Rev Cell Dev Biol 27, 1–27.
Nelson WJ (2003). Adaptation of core mechanisms to generate cell polarity. Nature 422, 766–774.
Nishio M *et al.* (2007). Control of cell polarity and motility by the PtdIns(3,4,5)P3 phosphatase SHIP1. Nat Cell Biol 9, 36–44.
O'Brien LE, Jou TS, Pollack AL, Zhang Q, Hansen SH, Yurchenco P, Mostov KE (2001). Rac1 orientates epithelial apical polarity through effects on basolateral laminin assembly. Nat Cell Biol 3, 831–838.
Olofsson SO, Boström P, Andersso l, Rutberg M, Perman J, Borén J (2009). Lipid droplets as dynamic organelles connecting storage and efflux of lipids. Biochim Biophys Acta 1791, 448–458.
Ooms LM, Horan KA, Rahman P, Seaton G, Gurung R, Kethesparan DS, Mitchell CA (2009). The role of the inositol polyphosphate 5-phosphatases in cellular function and human disease. Biochem J 419, 29–49.
Paternotte N, Zhang J, Vandenbroere I, Backers K, Blero D, Kioka N, Vanderwinden JM, Pirson I, Erneux C (2005). SHIP2 interaction with the cytoskeletal protein Vinexin. FEBS J 272, 6052–6066.
Pavio N, Battaglia S, Boucreux D, Arnulf B, Sobesky R, Hermine O, Brechot C (2005). Hepatitis C virus core variants isolated from liver tumor but not from adjacent non-tumor tissue interact with Smad3 and inhibit the TGF-beta pathway. Oncogene 24, 6119–6132.
Pesesse X, Deleu S, De Smedt F, Drayer L, Erneux C (1997). Identification of a second SH2-domain-containing protein closely related to the phosphatidylinositol polyphosphate 5-phosphatase SHIP. Biochem Biophys Res Commun 239, 697–700.
Pesesse X, Dewaste V, De Smedt F, Laffargue M, Giuriato S, Moreau C, Payrastre B, Erneux C (2001). The Src homology 2 domain containing inositol 5-phosphatase SHIP2 is recruited to the epidermal growth factor (EGF) receptor and dephosphorylates phosphatidylinositol 3,4,5-trisphosphate in EGF-stimulated COS-7 cells. J Biol Chem 276, 28348–28355.
Perlemuter *et al.* (2002). Hepatitis C virus core protein inhibits microsomal triglyceride transfer protein activity and very low density lipoprotein secretion: a model of viral-related steatosis. FASEB J 16, 185–194.
Phillipson M, Kubes P (2011). The neutrophil in vascular inflammation. Nat Med 17, 1381–1390.
Ploss A, Evans MJ, Gaysinskaya VA, Panis M, You H, de Jong YP, Rice CM (2009). Human occludin is a hepatitis C virus entry factor required for infection of mouse cells. Nature 457, 882–886.
Prasad N, Topping RS, Decker SJ (2001). SH2-containing inositol 5′-phosphatase SHIP2 associates with the p130(Cas) adapter protein and regulates cellular adhesion and spreading. Mol Cell Biol 21, 1416–1428.
Prasad NK, Tandon M, Badve S, Snyder PW, Nakshatri H (2008). Phosphoinositol phosphatase SHIP2 promotes cancer development and metastasis coupled with alterations in EGF receptor turnover. Carcinogenesis 29, 25–34.
Reiss S *et al.* (2011). Recruitment and activation of a lipid kinase by hepatitis C virus NS5A is essential for integrity of the membranous replication compartment. Cell Host Microbe 9, 32–45.
Rice CM (2011). New insights into HCV replication; potential antiviral targets. Top Antivir Med 19, 117–120.
Rodriguez-Boulan E, Paskiet KT, Sabatini DD (1983). Assembly of enveloped viruses in Madin-Darby canine kidney cells: polarized budding from single attached cells and from clusters of cells in suspension. J Cell Biol 96, 866–874.
Roe B, Kensicki E, Mohney R, Hall WW (2011). Metabolomic profile of hepatitis C virus-infected hepatocytes. PLoS One 6, e23641.
Shewan A, Eastburn DJ, Mostov K (2011). Phosphoinositides in cell architecture. Cold Spring Harb Perspect Biol 3, a004796.
Sleeman MW *et al.* (2005). Absence of the lipid phosphatase SHIP2 confers resistance to dietary obesity. Nat Med 11, 199–205.
Snooks MJ, Bhat P, Mackenzie J, Counihan NA, Vaughan N, Anderson DA (2008). Vectorial entry and release of hepatitis A virus in polarized human hepatocytes. J Virol 82, 8733–8742.
Stenzel N, Fetzer CP, Heumann R, Erdmann KS (2009). PDZ-domain-directed basolateral targeting of the peripheral membrane protein FRMPD2 in epithelial cells. J Cell Sci 122, 3374–3384.
Sumie S *et al.* (2007). Significance of glucose intolerance and SHIP2 expression in hepatocellular carcinoma patients with HCV infection. Oncol Rep 3, 545–552.
Trotard M, Lepère-Douard C, Régeard M, Piquet-Pellorce C, Lavillette D, Cosset FL, Gripon P, Le Seyec J (2009). Kinases required in hepatitis C virus entry and replication highlighted by small interference RNA screening. FASEB J 23, 3780–3789.
Wodarz A (2002). Establishing cell polarity in development. Nat Cell Biol 4, E39–E44.
Wu H, Feng W, Chen J, Chan LN, Huang S, Zhang M (2007). PDZ domains of Par-3 as potential phosphoinositide signaling integrators. Mol Cell 28, 886–898.
Wullschleger S, Wasserman DH, Gray A, Sakamoto K, Alessi DR (2011). Role of TAPP1 and TAPP2 adaptor binding to PtdIns(3,4)P2 in regulating insulin sensitivity defined by knock-in analysis. Biochem J 434, 265–274.
Xie J, Onnockx S, Vandenbroere I, Degraef C, Erneux C, Pirson I (2008). The docking properties of SHIP2 influence both JIP1 tyrosine phosphorylation and JNK activity. Cell Signal 20, 1432–1441.
Yu W, Shewan AM, Brakeman P, Eastburn DJ, Datta A, Bryant DM, Fan QW, Weiss WA, Zegers MM, Mostov KE (2008). Involvement of RhoA, ROCK I and myosin II in inverted orientation of epithelial polarity. EMBO Rep 9, 923–929.
Zhang J, Liu Z, Rasschaert J, Blero D, Deneubourg L, Schurmans S, Erneux C, Pesesse X (2007). SHIP2 controls PtdIns(3,4,5)P3 levels and PKB activity in response to oxydative stress. Cell Signal 19, 2194–2200.
Zwaenepoel K, Goris J, Erneux C, Parker PJ, Janssens V (2010). Protein phosphatase 2A PR130/B″alpha1 subunit binds to the SH2 domain-containing inositol polyphosphate 5-phosphatase 2 and prevents epidermal growth factor (EGF)-induced EGF receptor degradation sustaining EGF-mediated signaling. FASEB J 24, 538–547.